A Review on Optical Fiber Sensors for Environmental Monitoring

Hang-Eun Joe[1], **Huitaek Yun**[2], **Seung-Hwan Jo**[2], **Martin B.G. Jun**[2,#], **and Byung-Kwon Min**[1,#]

1 Department of Mechanical Engineering, Yonsei University, 50, Yonsei-ro, Seodaemun-gu, Seoul, 03722, Republic of Korea
2 School of Mechanical Engineering, Purdue University, 585 Purdue Mall, West Lafayette, IN, 47907-2088, USA
Corresponding Authors / E-mail: bkmin@yonsei.ac.kr
E-mail: mbgjun@purdue.edu

Environmental monitoring has become essential in order to deal with environmental resources efficiently and safely in the realm of green technology. Environmental monitoring sensors are required for detection of environmental changes in industrial facilities under harsh conditions, (e.g. underground or subsea pipelines) in both the temporal and spatial domains. The utilization of optical fiber sensors is a promising scheme for environmental monitoring of this kind, owing to advantages including resistance to electromagnetic interference, durability under extreme temperatures and pressures, high transmission rate, light weight, small size, and flexibility. In this paper, the optical fiber sensors employed in environmental monitoring are summarized for understanding of their sensing principles and fabrication processes. Numerous specific applications in petroleum engineering, civil engineering, and agricultural engineering are explored, followed by discussion on the potentials of OFS in manufacturing.

NOMENCLATURE

OFS = Optical fiber sensor

FBG = Fiber Bragg grating

LPFG = Long period fiber grating

MZI = Mach-Zehnder interferometer

MI = Michelson interferometer

FPI = Fabry-Perot interferometer

DAS = Distributed acoustic system

OTDR = Optical Time-Domain Reflectometry

OFDR = Optical frequency -Domain Reflectometry

BOTDA = Brillouin Optical Time Domain Analysis

BOFDA = Brillouin Optical Frequency Domain Analysis

RI = Refractive index

UV = Ultraviolet

Vis = Visible

NIR = Near infrared

SMF = Single-Mode fiber

MMF = Multi-Mode fiber

PCF = Photonic crystal fiber

HOF = Hollow optical fiber

CSF = Coreless silica fiber

DTS = Distributed temperature sensor

SHM = Structural health monitoring

1. Introduction

Environmental monitoring is essential in order to deal efficiently, safely, and effectively with resources, such as petroleum, natural gas, cultivated land, and others. To this end, various green technologies have been developed.[1] However, understanding and prediction of environmental changes remain challenges. Thus, unexpected changes that cause or become an ecological or human-health threat need to be monitored in the temporal and spatial domains.[2]

Monitoring technologies have been focused on analysis of the chemical and physical properties of environments.[3] Electrochemical sensors have been developed as monitoring sensors in various studies according to analytes[4-6] or sensing principles.[7-9] They have some advantages such as low-power operation, high selectivity, and the linear
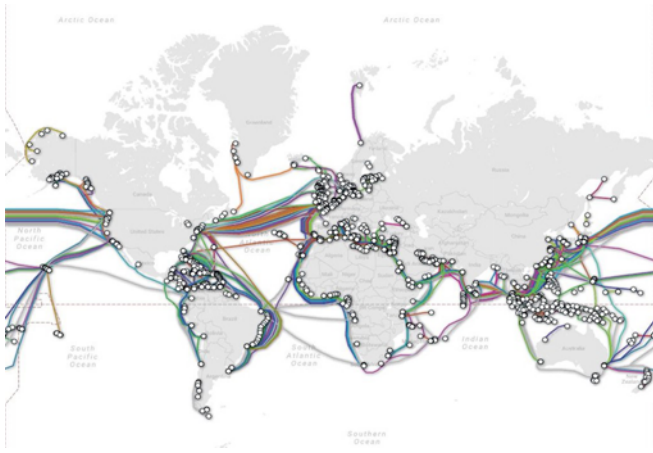
Fig. 1 Network map of submarine optical fiber cables[20] (Adapted from Ref. 20 on the basis of open access)

relationship between output signals and analyte concentration.[10] Electrochemical sensors generally contain the electrodes coated with a catalyst that promotes either oxidation or reduction of certain chemical species.[11] Even though they contain such high-selectivity catalysts, the study of catalyst species with high durability under extreme conditions of harsh environments remains challenging.[12] Other types of electronic sensors, for example electromechanical sensors[13] and thermoelectric sensors,[14] have also been studied as monitoring sensors in harsh environments. A micro-electro-mechanical sensor has been extensively studied owing to its small size[15] and low production cost.[16] However, those sensors have a short life-time in harsh environments due to the failure resulting from creep and plastic deformation, corrosion, and electrical disturbance.[17] Especially as environmental monitoring sensors are required to be running for long periods in harsh conditions, it is necessary to develop sensors that are durable in harsh environments for long operation times.

The optical fiber sensor (OFS) is a promising sensor for harsh environments. Compared with the electronic sensors, the OFS uses optical cables that have low heat loss and high data bandwidth over electric cables.[18] This allows connectivity over hundreds of thousands of kilometers via massive optical cables. Massive information technology resources are connected continent-to-continent[19] thanks to submarine cables laid around the world as shown in Fig. 1.[20] Optical fiber cables offer reliability even underneath the ocean for long durations, as optical fiber has unique characteristics such as immunity to electromagnetic interferences and chemical corrosion, and low heat loss.[21] This indicates that the OFS can also generate and transmit measurement data with high sensitivity even in harsh ambient conditions, such as in downholes for oil recovery[22] and in nuclear power plants.[23] Moreover, the OFS is compatible with existing fiber-optic communication systems, which means environmental monitoring using the OFS can be remotely operated in a network operating system.[24]

The light weight, small size, and high flexibility of optical fibers play an important role in environmental monitoring sensors as well. They enable the installation of OFS at sensing sites with complicated structures such as pipelines[25] and ice shelves.[26] OFS for ground monitoring are laid on the ground or underground to analyze physical or chemical changes such as produced by

landslides,[27] earthquakes,[28] and soil fertility.[29] As the OFS is flexible enough to be attached to complicated structures at sensing sites, it can provide the temporal and spatial distributions of environmental properties.[30]

The purpose of this paper is to review OFS types that have been employed for environmental monitoring purposes. In Section 2, the principles of those types are summarized in two categories: the point-based OFS and the distributed OFS. In Section 3, the sensor fabrication processes are described according to three categories: grating inscription, functional coating, and fiber shaping. In Section 4, a variety of OFS types used for environmental monitoring in the fields of petroleum engineering, civil engineering, and agricultural engineering are explored and their potentials in manufacturing are discussed. In Section 5, conclusions are drawn.

2. Principles of OFS

2.1 Point-Based OFS

A point-based OFS produces measurement data at certain locations according to where its specific sensing components are. Each sensing component responds to a stimulus caused by changes of the environmental properties at its location, so that the measurement data are directly generated at the sensing location. Accordingly, the point-based OFS provides measurement data with high sensitivity and selectivity. The point-based sensor has a variety of configurations such as Fiber Bragg Grating, Long-Period Fiber Grating, the Mach-Zehnder interferometer, the Michelson interferometer, the Fabry-Perot interferometer, and the Sagnac interferometer.

2.1.1 Fiber Gratings

The Fiber Bragg Grating (FBG) was introduced by Hill et al. for the first time.[31] They found that the periodic gratings at the core of an optical fiber were used as a narrowband reflector. Since then, FBG-based sensors have been extensively investigated according to fabrication methods, principles, and applications.[32] The periodic gratings are generally formed by refractive index (RI) changes using various methods such as ultraviolet or CO_2 laser irradiation,[33,34] ion implantation,[35] electric arc,[36] chemical etching,[37] and mechanically induced fiber deformation.[38] Fig. 2 shows a schematic of the FBG structure and its spectral responses. The periodic gratings formed at the core of the optical fiber induce light reflection at a certain wavelength, and all of the other wavelengths of light are transmitted. The Bragg wavelength (λ_B), the central wavelength of the reflected light, is described as $\lambda_B = 2n\Lambda$, where n is the effective RI and Λ is the periodicity of the gratings. The FBG has a periodicity of gratings within a few hundreds of nanometers for the reflected light around telecommunication wavelengths.[39] For the FBG sensor, the Bragg wavelength is sensitive to changes in environmental properties such as temperature (T) or strain (ε). The shift of Bragg wavelength is described as

$$\Delta\lambda_B \,/\, \lambda_B = \kappa_S \cdot \varepsilon + \kappa_T \cdot \Delta T \qquad (1)$$

where κ_S and κ_T are strain and temperature constants, respectively.[40] As described by Eq. (1) temperature and strain affect the Bragg
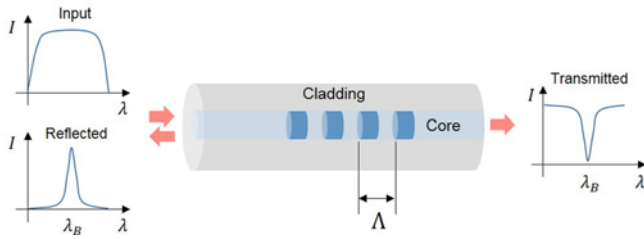
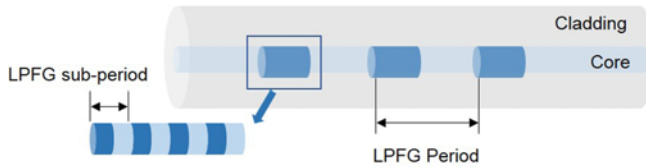Fig. 2 Schematic of FBG structure and spectral response
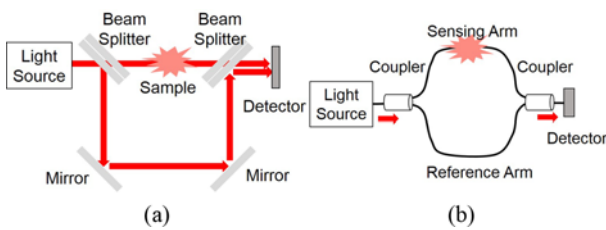

Fig. 3 Schematic of LPFG structure

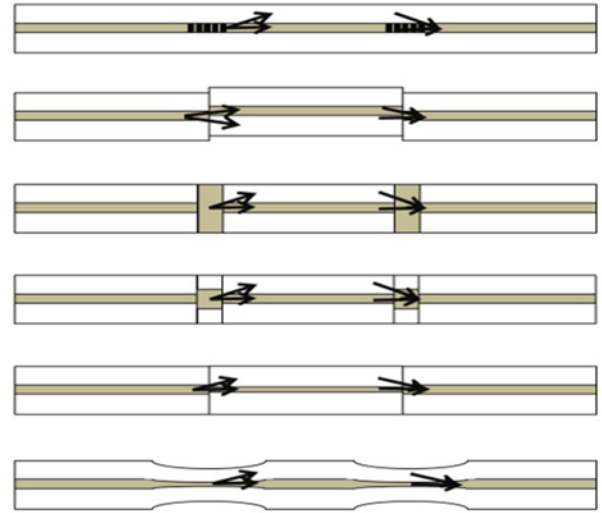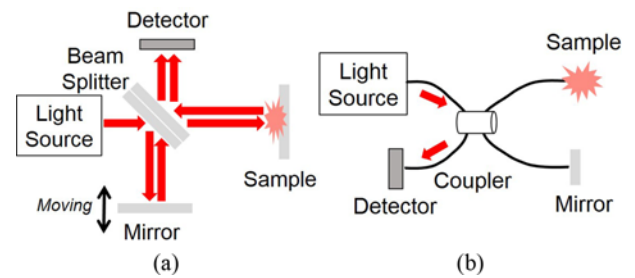Fig. 4 Dagrams of (a) MZI sensor and (b) fiber-optic MZI sensor

Fig. 5 In-line MZI sensors using various optical fibers[48] (Adapted from Ref. 48 with permission)

Fig. 6 Diagrams of (a) MI sensor and (b) fiber-optic MI sensor

wavelength, so that it is difficult to discriminate two parameters using a single FBG. In many researches, two different gratings or fibers are used to decouple temperature and strain.[41]

The Long-Period Fiber Grating (LPFG) is the periodic grating that has a periodicity within a few hundreds of micrometers, which is longer than that of the FBG.[42] Fig. 3 illustrates the general LPFG structure. The LPFG couples the light from a guide mode into a propagating cladding mode at a certain wavelength,[43] so that it acts like a wavelength-dependent loss element. The LPFG is used not only temperature sensors but also bending sensors.[44]

2.1.2 In-line Interferometer

The Mach-Zehnder interferometer (MZI) using optical fibers is a flexible platform for environmental sensing applications.[45] As shown in Fig. 4, the basic configuration of the MZI sensor is based on light transmission and interference. The light from a single light source is divided by the first coupler in two optical fibers: a sensing arm and a reference arm (see Fig. 4(b)). The sensing arm is exposed to the environments to be measured. The light propagating in the two paths is recombined at the second coupler. Then, the relative phase difference between the lights propagating in the two arms induces interference signals of the combined light. The interference signals contain the optical information of the environmental properties.

As interest in the miniaturization of the optical-fiber-based MZI sensor has increased, in-line configurations have been developed in various studies.[46,47] Whereas the bulky configurations use beam splitters or couplers to divide and recombine the light, in the in-line MZI sensor, contacts formed by splicing different optical fibers are used for dividing and recombining the light. As shown in Fig. 5, various types of in-line MZI sensors have been designed using FBG or LPFG, the single-mode fiber (SMF), the multi-mode fiber (MMF), the coreless silica fiber (CSF), and tapered fibers.[48] The coupler part in the in-line MZI is the contact formed by splicing two different fibers with respect to their core size,[49] core type,[50] or cladding size.[51] The divided light at first contact individually propagates in the core mode and the cladding modes. The core and cladding of optical fiber correspond to a reference arm and a sensing arm, respectively. At the second contact, the light in the core and cladding modes are recombined. The relative phase difference (Φ) of those two modes is described as

$$\Phi_{m} = (2\pi \cdot \Delta n_{\text{eff}}^{m} \cdot L) / \lambda \qquad (2)$$

where $\Delta n_{\text{eff}}^{m}$ is the effective refractive index between the core mode and the mth cladding mode, L is the interaction length between the two contacts, and λ is the wavelength of the incident light.[52]

The Michelson interferometer (MI) using optical fiber is also based on the relative phase difference of the light propagating in two paths.[53] As shown in Fig. 6, the light reflected from the environment and the light reflected from a reference mirror are combined to form the
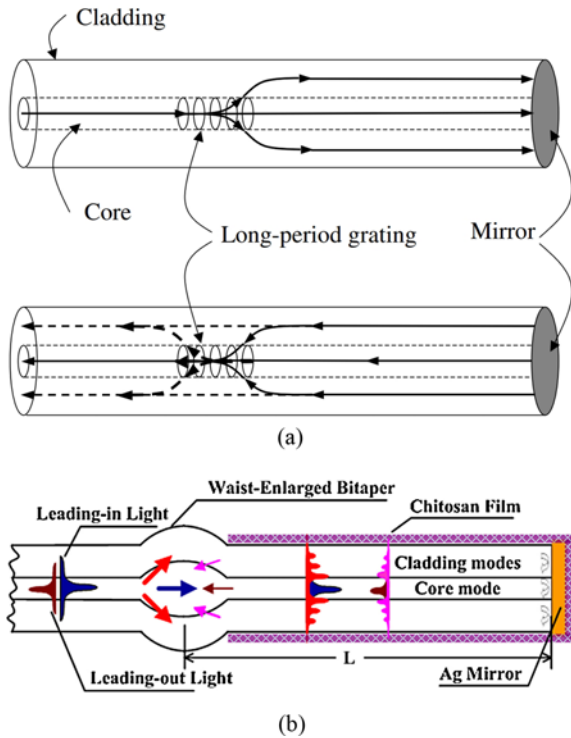
Fig. 7 Examples of in-line Michelson sensors[55,56] (Adapted from Ref. 55 and 56 with permission)
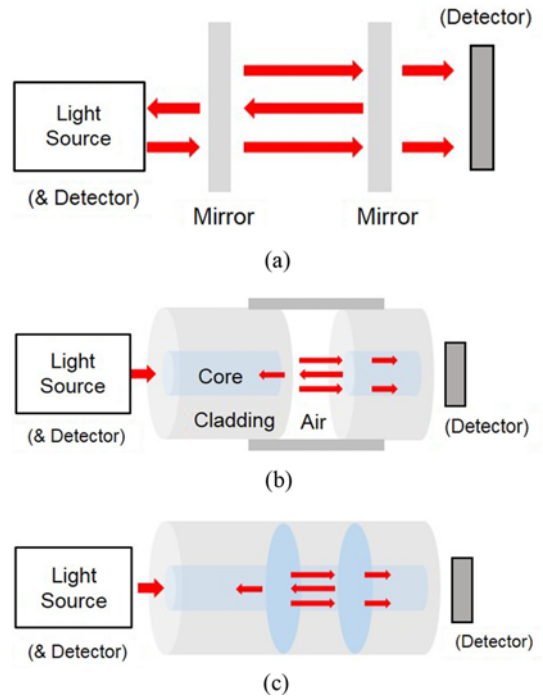

Fig. 8 Diagrams of (a) FPI sensors and fiber-optic FPI sensors with (b) intrinsic type and (c) extrinsic type

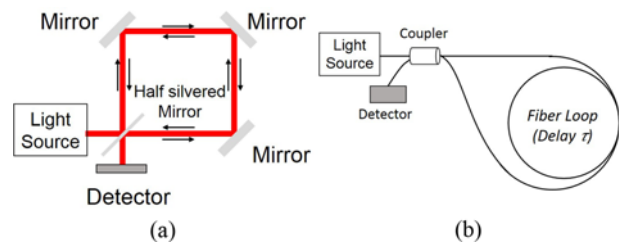Fig. 9 Diagrams of (a) Sagnac interferometer and (b) fiber-optic Sagnac interferometer

interference signals. Whereas the MZI sensor is based on the transmission mode, the MI sensor generates interference signals based on the reflection mode.

The in-line MI sensors also consist of various types of optical fibers such as the LPG, SMF, PCF, and tapered fiber. The contact between two different optical fibers is used as a coupler to divide or recombine light, similarly to the in-line MZI sensor. Unlike the MZI however, the MI sensor has a mirror element to induce total reflection at the end of the fiber, as shown in Fig. 7. The relative phase difference of the core and cladding modes is similar to that of the MZI sensor as in Eq. (2). Note that, in the case of the MI sensor, L is the length of the interferometric cavity, which is the space between the contact of the two fibers and the mirror at the end of the fiber.[54]

The Fabry-Perot interferometer (FPI) using optical fiber consists of two reflection mirrors (see Fig. 8(a)) instead of couplers. An optical cavity formed between the two mirrors is the main part of the FPI sensor for generation of interference signals.[57] The FPI sensors has been categorized in two types: the intrinsic type and the extrinsic type, as shown in Figs. 8(b) and 8(c). In general, the optical cavity of the intrinsic FPI is the optical fiber, whereas the optical cavity of the extrinsic FPI is an air-gap. Those cavities are formed in the middle by splicing the fibers or at the end using a mirror either.[58]

The interference signals of the FPI sensor are formed by the reflected light at both end surfaces of the cavity. As physical characteristics of the environment (e.g., temperature, pressure, displacement, and stress) change, the length or refractive index of the cavity becomes deflected.[59] The deflected cavity induces a phase shift in interference signals. For example, in the case of pressure, the change in cavity length ΔL due to the pressure difference may be expressed as

$$\Delta L = 3a^4 \cdot \Delta P \cdot (1 - \upsilon^2) / 16E \cdot d^3 \qquad (3)$$

where a is the radius, P is the pressure, υ is the Poisson ratio, E is the Young's modulus, and d is the diaphragm thickness.[60] The Sagnac interferometer was first introduced by Monsieur Sagnac in 1913.[61] As in other interferometers, the relative phase difference of the light propagating in two paths is used to obtain the optical information of the environments. The incident light is divided into two beams that travel the same pathway in opposite directions. Fig. 9 shows a schematic of Sagnac interferometers. In general, a fiber-optic Sagnac interferometer is developed for a fibre-optic gyroscope based on a rotational seismometer.[62] The optical path length difference (Δx) caused by the light rotation loop is described as
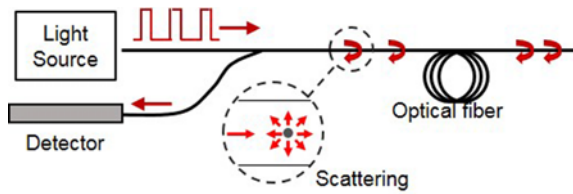
Fig. 10 Schematic of distributed OFS with light-backscattering

Table 1 Measurement performances of distributed sensing methods[67]

Sensing technology	Sensing range	Spatial resolution	Main measurements
Raman OTDR	1 km	1 cm	Temperature
	37 km	17 m	
Brillouin OTDR	20~50 km	~ 1 m	Temperature and strain
Brillouin OTDA	150~200 km	2 cm (2 km extension)	
		2 m (150 km extension)	
Rayleigh OFDR	50~70 m	~ 1 mm	

$$\Delta x = \Omega \cdot R \cdot \Delta t \qquad (4)$$

where Ω is the rotation rate, R is the radius of the loop and Δt is the time for the light beam to travel the loop.[61] In environmental monitoring, Sagnac interferometers have been used for vibration and acoustic detection in extremely rugged environments because they have no moving parts. For example, earthquake monitoring by Sagnac interferometers has been widely studied.[63]
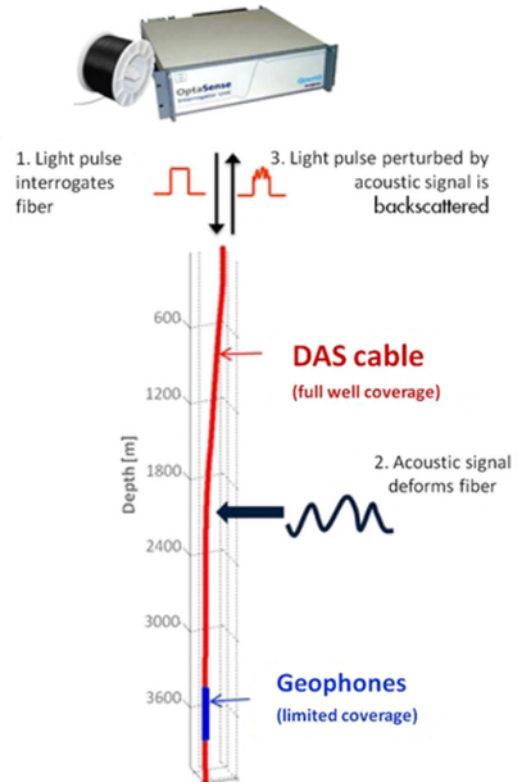
2.2 Distributed OFS

Unlike the point-based sensors, the distributed OFS produces the measurement data of the spatial and temporal domains across long distances. As shown in Fig. 10, for the distributed OFS, the light source is incident in one end of the fiber, and the other side is freestanding. The distributed OFS detects the light-backscattering induced at any points located on the optical fiber. Although the fiber is broken in the middle, frequency-based analysis is achieved for the remaining fiber.

There are two types of distributed OFS: Optical Time-Domain Reflectometry (OTDR) and Optical Frequency-Domain Reflectometry (OFDR).[64] The incident light has short pules of a certain frequency in the OTDR, whereas in the OFDR, the incident light illuminates by frequency sweeping using a tunable laser.[65] Compared with the OTDR, the OFDR has high special resolution, signal stability, dynamic range, and interrogation time.[66] The main principle of those types is that changes in environmental properties such as vibration and pressure, generate the scattered light. This enables monitoring of environmental changes within a large measurement range in both the temporal and spatial domains.

Distributed OFS are categorized according to collision type and frequency range: Rayleigh scattering, Brillouin scattering, and Raman scattering. Table 1 shows the performances of the different distributed sensing techniques.[67]

2.2.1 Rayleigh Scattering

Rayleigh scattering is an elastic scattering caused by interactions between the incident light and the impurities of the fiber core.[68] As

Fig. 11 Schematic of distributed OFS for vertical seismic profiling[70] (Adapted from Ref. 70 with permission)

energy of the photons in the incident wave is preserved, the scattered light has the same frequency as the incident light. The scattered light is sensitive to the external stimulus, such as a magnetic field, bending of the fiber, and uniaxial pressure.[64] Accordingly, the Rayleigh scattering sensor is used for vibration, strain, and temperature measurement. For example, similar to other acoustic wave sensors,[69] an external acoustic wave causes a change at the sensing point, in the case of optical fiber, back-scattered light is induced as shown in Fig. 11.[70] The distributed acoustic system (DAS) is used to obtain underground information for the oil and gas industry.

2.2.2 Brillouin Scattering

Brillouin scattering is an inelastic scattering caused by an acoustic wave from lattice vibration. The scattered light has a lower frequency than that of the incident light, because the incident photon absorbs the vibration energy of the phonon. The frequency shift that occurs by Brillouin scattering depends on thermal or mechanical deformation due to the stress-optical effect.[71] Brillouin scattering based sensors are categorized as the Stimulated Brillouin Optical Time-Domain Analysis (BOTDA) and the Spontaneous Brillouin Optical Time-Domain Reflectometry (BOTDR). The BOTDR analyzes both the frequency shift and intensity change of scattered light, but the intensity has weaker signals than the frequency.[72] The BOTDA measures the gain from two waves that are illuminated at both ends.[73] However, it does not run when the loop is broken at any point of the fiber, whereas the BOTDR runs even if the fiber is broken. Thus, a single ended BOTDR system has been widely studied for industrial applications.[74]
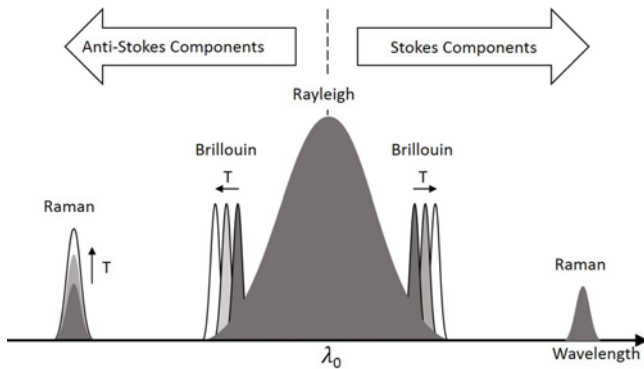
Fig. 12 Temperature dependencies of back-scattered optical signals

Fig. 13 Schematic of system for femtosecond laser machining of LPFG[84] (Adapted from Ref. 84 with permission)

2.2.3 Raman Scattering

Raman scattering is another inelastic scattering, which induces a shift of wavelength interrelated with the stretching modes between atoms.[75] Raman scattering largely depends on the temperature changes surrounding the distributed OFS.[67] Raman scattering has two types: Stokes Raman scattering and anti-Stokes Raman scattering. Fig. 12 illustrates the temperature (T) dependencies of Stokes and anti-Stokes Raman scattering.

Stokes Raman scattering causes the incident photons to lose their energy owing to interaction between molecular the vibrational modes at the optical fiber, so that the scattered light has a longer wavelength. In contrast, anti-Stokes Raman scattering causes the incident photons to absorb the energy induced from the interaction between the vibrational modes. Hence, anti-Stokes Raman scattered light has a shorter wavelength. When the environmental temperature increases, the molecules of the distributed OFS are thermally excited. Since the incident photon absorbs the excited energy, anti-Stokes Raman scattering is sensitive to temperature changes. The incident light absorbs the energy of the excited phonons, which induces and increase of the amplitude of the anti-Stokes Raman scattering signal only. Thus, ratios of Stokes to anti-Stokes Raman scattering signals are measured for temperature monitoring.[76]

3. Sensor Fabrication Processes

3.1 Grating Inscription

FBGs are typically fabricated by laser inscription that induces change of material properties such as such as the RI, thermal conductivity, specific heat, and phase transition of the material.[77] For FBG fabrication, laser irradiation is used for RI changes permanently at the fiber core. There are several types of lasers used in manufacturing fields.[78] An ultraviolet (UV) laser is a traditional process for FBG fabrication, which is limited to a photosensitive fiber. Hydrogen doping is used to enhance durability of the FBG fiber fabricated the UV laser.[79] Recently, a femtosecond laser inscription technique has been reported on for a decade.[80] Femtosecond laser irradiation induces ionization and non-linear absorption at the fiber core, which change the RI permanently by phase or structural modification.[81] Accordingly, the femtosecond laser technique can be used for non-photosensitive fibers. Moreover, RI change at the fiber core is achieved without stripping of outer coatings.
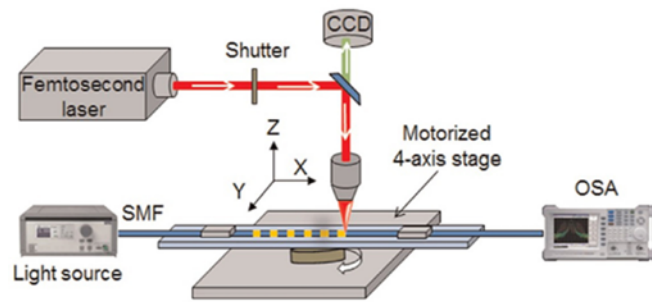
Several inscription process is generally used to fabricate the periodic gratings. The periodic pattern is generated by diffraction pattern with over 1st order diffraction generated from a phase mask.[82] FBGs offer high repeatability appropriate for mass production; however, the drawback is collision due to the short distance between the fiber and the phase mask. In order to avoid collision between the fiber and phase mask, Talbot interferometer that consists of mirrors or silica blocks is proposed.[40] Another common method is interference lithography, because it is a fast method for forming periodic gratings over a large area. However, gratings with complicated shapes are difficult to fabricate by interference lithography or phase mask.

Meanwhile, as another improvement, the direct writing method based on femtosecond laser has been proposed. It allows that the optical fiber is accurately adjusted by a piezo linear stage in order to increase the grating length and generate of gratings with complex shapes.[83] Fig. 13 illustrates an example of the system for femtosecond laser machining of LPFGs.[84] This method is flexible for control of the shape of gratings, and the expansion error is only few micrometers. Likewise, several direct writing techniques based on femtosecond laser are widely studied to fabricate FBG sensors.[85,86]

3.2 Functional Coating

Thin film coating has been widely studied for improvement of the sensitivity and selectivity of OFS in monitoring of the environmental properties such as the concentrations of carbon dioxide[87] and hydrogen,[88] humidity,[89,90] and pH.[91] Fig. 14 shows typical types of coatings on OFS.[88] Those functional coatings change the optical property of the propagating cladding mode, so that the OFS becomes more sensitive. In general, coatings are used to improve selectivity or sensitivity of the optical fiber sensors. Metal oxide sensing layer has widely studied. For example, a perovskite $La_{0.3}Sr_{0.7}TiO_3$ laser was proposed to discriminate H_2 and CO_2 with a monotonic concentration.[92] Zinc oxides (ZnO) or platinum-nanoparticle-incorporated graphene oxide was proposed to detect ammonia gas selectively.[93,94] For a metal film coated at the fiber, it also works as a reflector based on surface plasmon resonance and FPI.[95]

Physical vapor deposition (PVD) is a common process utilized to deposit thin film with high purity and durability. It has various sub-processes, such as thermal/e-beam evaporation, magnetron or ion sputtering, molecular beam epitaxy, and pulsed laser deposition.[95] PVD is achieved in a vacuum chamber to form film with physical collision
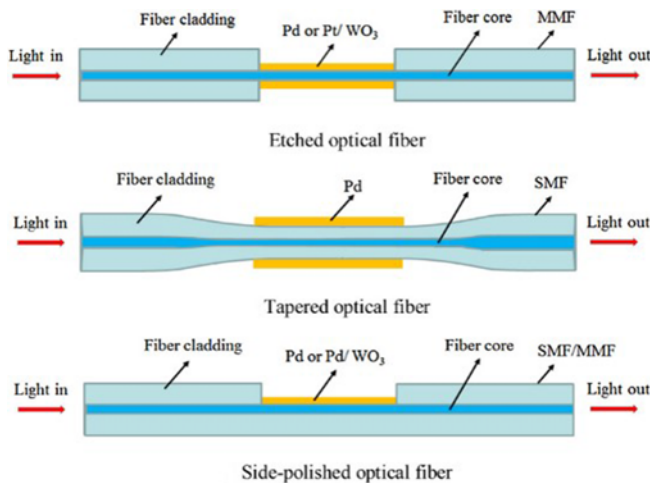
Fig. 14 Various types of OFS for detection of hydrogen[88] (Adapted from Ref. 88 with permission)

Fig. 15 Diagram of optical fiber shaping processes: (a) direct machining, (b) tapering, and (c) side-polishing

between the target (optical fiber) and coating materials. Thus, OFS coated with thin film by PVD processes have been widely studied because the PVD processes provide high purity, good adhesion, and high durability.[89,96,97] However, most PVD processes are limited to flat surfaces, due to step-coverage issues.[98] Chemical vapor deposition (CVD) is another process for deposition of thin film on three-dimensional targets, such as the peripheries of optical fiber.[98] The main principle of CVD processes is a chemical reaction between gas mixtures, but the chemical reaction between gas precursors and the optical fiber has to be prevented.[99] Recently, atomic layer deposition has emerged as alternative, as it provides better conformity and thickness control on an atomic scale.[100,101]

3.3 Optical Fiber Shaping

There are several shaping techniques that can enhance optical fiber sensitivity: Direct machining, tapering, side-polishing, and splicing. Direct machining is employed to fabricate micro/nano-patterns at the OFS. Focused ion beam (FIB) is mainly used as a direct-writing tool.[102] Fig. 15(a) shows a diagram of the direct machining by FIB. Andre et al. fabricated the gap in the optical fiber by FIB in order to use as an optical cavity of the fiber-optic FPI.[103] Kou et al. fabricated a smallest fiber tip grating by FIB machining.[104] The micro/nano-patterns at the OFS have been proposed for OFS performance improvement.

Tapering method is used to fabricate the tapered fiber that has different core and cladding diameters from those of the original fiber. Fibers are tapered by a heat source and an axial force to make them longer. Fig. 15(b) shows a diagram of the fabrication process for fiber tapering. Ahmed et al. fabricated the tapered fiber by pulling both the ends of the fiber along the fiber-axis and heating the middle of the fiber simultaneously.[105] There are lots of commercial fusion splicer and laser splicer to fabricate the tapered fibers. Although the tapered fiber have a little transmission loss, it have much stronger interaction between evanescent fields and target materials.

Side-polishing of the fiber is a fabrication process to improve performance of the OFS as well. Side-polished fiber enables the evanescent field to reach the target material directly. Fig. 15(c) shows
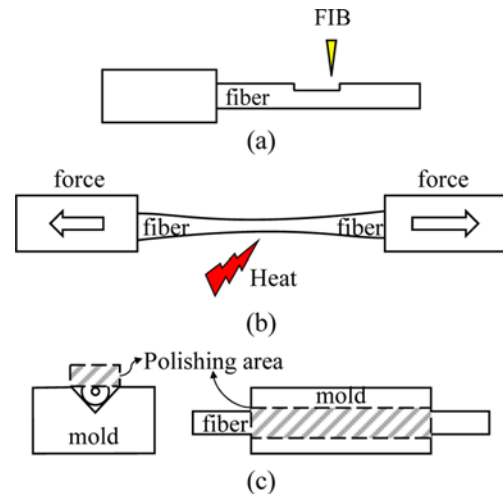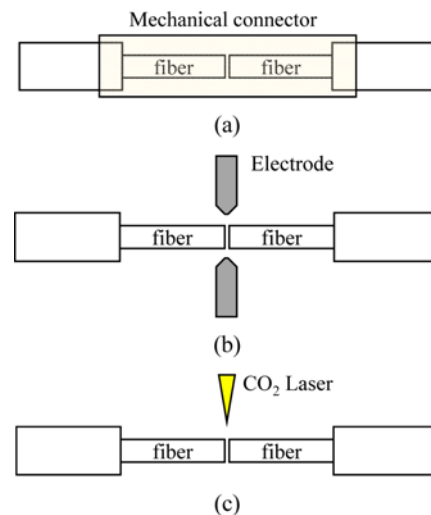
Fig. 16 Diagrams of optical fiber splicing processes: (a) mechanical splicing, (b) Arc fusion splicing, and (c) laser splicing

a basic concept of the polishing process. Tseng et al. introduced the side-polishing method. One side of the fiber is polished to make the leaked light at the polished area to access the target directly.[106] The side-polished fibers based on SMF or PCF were also studied to measure chemical properties.[107,108]

One other technique for OFS sensitivity enhancement is splicing. There are three methods of fiber splicing: mechanical splicing, fusion splicing, and laser splicing. Fig. 16 depicts the basic concepts of three splicing techniques. They each have their own advantages and disadvantages. Mechanical splicing uses an alignment device for firmly griping the two fibers (see Fig. 16(a)). This is a simple and easy method, but it typically incurs higher transmission loss. Fusion splicing is achieved by a permanent welding with a heating source. The fiber splicing is categorized according to the heat source such as Arc fusion splicing, filament splicing, flame splicing, and laser splicing.[109] The Arc fusion splicing is commonly employed to splice the fibers because it is fast and cost-effective (see Fig. 16(b)). The filament splicing is

conducted by the resistance heater surrounding the fibers. It is employed for specialty fibers or the fiber required high splice strength. Other splicing techniques have been studied to improve the transmission loss and to provide more functionalities such as tapering, lensing, other glass-shaping operations, and splicing as well. The laser splicing provides high resolution for enhanced heating position control (see Fig. 16(c)). It allows to fabricate the special fibers composed of different types of fibers such as SMF and MMF, SMF and PCF, or SMFs with different core diameters. For example, Chong et al. suggested an effective method that uses a CO_2 laser to splice PCF and SMF in order to improve a transmission loss.[110]

4. Trends in OFS for Environment Monitoring

4.1 OFS in Petroleum Engineering

Oil and gas industry assets, such as pipes, pumps, joints, and so on, are required to be monitored.[111,112] If they get damage due to natural disasters or human intervention, not only are resources lost, but surrounding environment can become polluted. The assets are placed in the sea bottom or downhole under high-pressure, high-temperature environments and immersed in corrosive brine.[113,114] In the case of delivery pipes, they are spread over kilometers and buried underground.[115] Pipeline leakage occurs due to various causes such as fatigue and vibration by fluids, buckling of vertical pipelines in subsea structures, and corrosion by soil or inner contents. When leakages happen on a pipeline, various events follow such as negative-pressure waves, acoustic noise from turbulent flow, the temperature gradient or displacement of the soil.[116] Distributed OFS is employed to monitor these causes and results so that leakage can be prevented at earlier stages.[117]

A variety of distributed OFS are studied and used in the field for their high strength and easy installation, high durability, and long measurement range. Temperature or acoustic signal sensing for pipeline-leak-monitoring is achieved by a variety of distributed OFS such as OTDR,[118] OFDR,[119] BOTDA,[120] and BOTDR.[121] Corrosion monitoring of an internal pipeline was achieved by distributed OFS wound around the pipe because the pressure applied to internally corroded pipes causes the hoop strain.[122] Those distributed OFS can be used to identify and convey warnings (in the form of pre-alarms) of leakage possibilities.[123] Distributed OFS for vibration monitoring has been also investigated. Peng et al. proposed a phase-OTDR that can sense intrusion over the range of 131.5 km with a resolution of 8m.[124] Tan et al. also used phase-OTDR along with support vector machine to discriminate signals of artificial digging, mechanical excavation, and car crossings.[125] Similarly, Tejedor et al. used phase-OTDR and monitored machine activity and any threats near a pipeline in a field trial as shown in Fig. 17.[126]

In addition to distributed OFS, point-based OFS using the FBG have been studied for pipeline monitoring due to the fact that they, with their higher sensitivity than that of the distributed type, can be multiplexed along a pipeline.[127] Freire et al. measured strain after the repair of a pipeline with composite material.[128] In leakage detection, the negative-pressure method is used. It measures the pressure difference between two points using FBG sensors instead of electronic sensors.
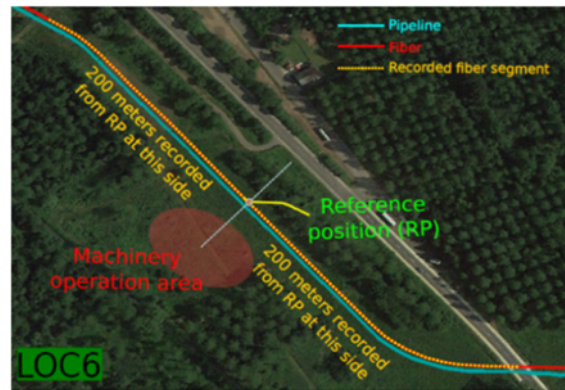
Fig. 17 A field trial of threat monitoring using phase-OTDR technique[126] (Adapted from Ref. 126 with permission)
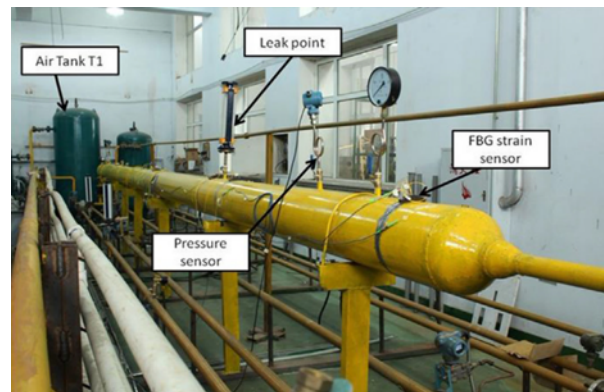
Fig. 18 Lab-experiment setup for detection of pipeline leakage[130] (Adapted from Ref. 130 with permission)

Fig. 18 shows the system setup to verification of pipeline leakage using FBG sensors with the negative-pressure method.[129,130] The strain along the pipe cross-section is measured to detect leaks from natural gas pipelines. FBG sensors were also investigated to measure vortex-induced vibration inside the pipe,[131] the hoop strain of a PVC pipe,[132] stress and strain of buried pipelines,[133] and criminal activity such as drilling.[134]

To mitigate climate change, storing of the CO_2 gas underground has been proposed, which is termed as Carbon Capture Storage (CCS).[135] Several countries are working on CCS projects, which include the Otway project in Australia, the Janggi and Pohang Basin in South Korea, seven CCS sites in the US, the Sulcis basin in Italy, Alberta in Canada, and others. OFS is promising not only as a direct measurement method but also for its long-range sensing capability in high-pressure and high-temperature environments. Bao et al. measured CO_2 in brine at sequestration pressure (1400 psi).[136] Melo et al. coated polystyrene on LPG to measure CO_2 concentrations at high pressure (1400 lbf/in^2), in the lab environment.[87] Commercial distributed-type sensors measure the pH change of underground water when CO_2 gas is smeared into it, but no robust monitoring in the actual field has yet been reported.[137] Further field research into CCS leak monitoring is expected in the near future.

Fig. 19 Drilling riser system with FBG sensors[142] (Adapted from Ref. 142 with permission)

Fig. 20 Schematic of distributed temperature sensing of ice shelf with two boreholes[152] (Adapted from Ref. 152 with permission)

As oil sources underground deplete, those in the sea bottom are being developed. Subsea-structures including pumps, umbilical lines, and pipes usually are subject to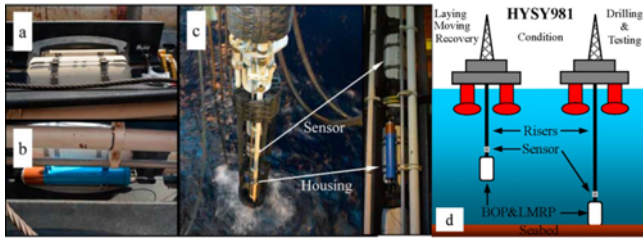 high thermal stress due to the required large pressures. Therefore, temperature monitoring of these structures is vital to the maintenance of subsea oil reservoirs.[114] Subsea-structure monitoring using OFS requires specific components such as wet mate connectors and fiber-optic rotary joints, which incur significant insertion and return loss. This results in limited range and data loss at farther positions. Ravet et al. proved that the Stimulated BOTDA is not affected by those components; they also demonstrated that, relative to the Raman OTDR or BOTDR, it has a lesser dead-zone and is robust to fiber aging.[114] This system can measure temperature and strain with 10 μm strain and 0.5°C temperature resolution over the span of a 50 km distance at a spatial resolution of 2 m. Among the systems field implementation are power umbilical and heated flow lines for monitoring of temperature distribution. Gyger et al. tested an ultra-long range (> 300 km) distributed OFS system that can be used in subsea pipe monitoring.[110] Feng et al. used BOTDA to monitor upheaval buckling in buried subsea pipelines.[138]

A variety of point-based OFS also have been investigated to monitor the integrity of subsea structures. Post-installable deep-water flow-line strain-monitoring sensors based on FBG were proposed.[139,140] The adhesive clamp allows easy installation and protection of FBG sensors in subsea environment. Razali[141] embedded FBG sensors to a full composite epoxy sleeve reinforcing an offshore oil and gas pipeline. The epoxy grout protects the fiber sensors. The epoxy contributes to pipeline strengthening but was difficult to attach other types of sensors. Xu et al. measured stress and bending movements in a drilling riser using four FBG sensors as shown in Fig. 19.[142]

In downhole fiber sensors induce differential attenuations when the fiber undergoes physical or chemical perturbations such as bends, compressions, and chemical contamination.[143] Hydrogen darkening is a common problem in oil well at high temperature. Although a combination of hermetic coating, tailoring of the glass properties, and the double-ended configuration[144,145] are studied to overcome the hydrogen darkening problem, but, it is still challenging.

There are demands to monitor hydrogen as a new type of energy resource because of its highly flammable and explosive nature. Westerwall et al. coated an Pd-Au sensing layer onto the end of an optical fiber for detection of hydrogen concentrations up to 250 mbar at room temperature.[146] Jiang et al. designed an FBG hydrogen sensor with its side-polished and sputtered with Pd and Ti to make it sensitive to curvature strain.[147] Poole et al. proposed a D-shaped hydrogen OFS
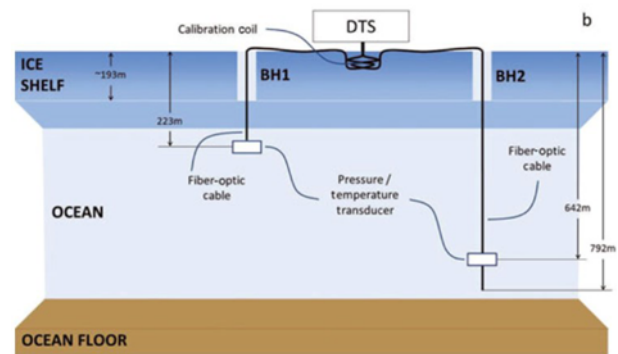
with palladium nanoparticle infused metal oxide film for improved conductivity.[148] This OFS can detect hydrogen concentrations of up to 10% at temperatures over 500°C. Huang et al. discovered that a Pd-Y-alloy coating for an optical fiber hydrogen sensor as well.[149]

4.2 OFS in Civil Engineering

In geohazards monitoring, distributed OFS are widely used to detect landslides, earthquakes, dam and dike conditions, and temperatures over large areas. Because ground monitoring requires a capability of covering large areas, distributed OFS are typically used in this field. Landslides are often caused by heavy rainfall that penetrates and softens soil, thereby rendering it unstable and causing it to fail under shear stress. To prevent disasters of this kind, early detection of soil movement, crucially, can provide enough time for evacuation. The BOTDR is one of the monitoring techniques that are used to detect early signs of movement. The heavy-rains-caused landslides in Gansu, China, was monitored by the distributed OFS.[64] In addition, water seepage detection by distributed OFS is a major principle of landslide early warning. Zhu et al. found that water seepage significantly effects ground to stability.[150] Earthquake monitoring is one of the applications of fiber sensors. In earthquake monitoring, physical features such as heat flow, displacement, and seismic waves are measured. Seismic waves, with their high resolution and accuracy, are considered to be one of the most effective methods for prediction of earthquakes.[151] Strong candidates for detection of seismic waves are OFS based on Sagnac interferometers. Kurzych et al. proposed an autonomous fiber-optic rotational seismometer based on the Sagnac effect.[62]

Distributed OFS is also used to temperature monitoring of large areas such as ice shelves. Tyler et al. employed the distributed temperature sensor (DTS) system to monitor the temperature of Antarctic ice shelves and a sub-ice-shelf cavity, as shown in Fig. 20.[152] The DTS system was installed on the ice shelf, and an optical fiber was reached to the sub-ice-shelf through a borehole. Kobs et al. also utilized the DTS, in their case to measure basal melting of ice shelves in order to better understand climate change. They installed DTS and the optical cable through the Antarctic ice shelf to a depth of 600 m so as to measure the temperature of the ice shelf cavity.[26]

Another utilization of distributed OFS is dam or dike monitoring. Once a dam or dike is built, one of the main concerns is water seepage

which can damage it and eventually cause structural failure. This failure is caused either internally or externally. The detection of a change in temperature caused by invading water is the key principle in this field. To address this problem, the DTS has been utilized by installing fibers inside dams and dikes. However, detection of seepage with temperature measurements is quite complex. First, there is the temperature difference between the normal state and the water-seepage state. Second, there are many other factors that affect the temperature of the structure such as seasonal temperature variations or exposure to the sun or weather. There are two major solutions. As a passive solution, there is temperature-contrast enhancement by installing several distributed OFS both on the reservoir side and downstream. As an active solution, the temperature-difference contrast can be enhanced by measuring thermal conductivity with a wire heater as well as DTS.[64] This principle is almost the same as that of distributed thermal perturbation sensing which is widely used in borehole thermal logging. Rosolem et al. proposed fiber ring sensors with the elastomeric membrane coating for dam, tank, and reservoir water-level monitoring.[153] Unlike distributed fiber sensors, which should be planned for and installed during construction of dams, this sensor can be installed any time it is needed. Its installation, moreover, is easy and inexpensive.

Structural health monitoring (SHM) is utilized to diagnose structural and environmental parameters and, accordingly, warn of unexpected accidents in conducting sound safety management.[154,155] Sensors in this field should have the capability of monitoring status parameters and influential environmental parameters simultaneously. Distributed fiber sensors have a great potential for structural health monitoring due to their inherent distributive nature. Some examples of SHM for green technology are the monitoring of structural devices for renewable energy generation and materials for better fuel efficiency and reduced emissions. The structural devices used in renewable energy fields require ever-more power are growing larger in size all the time. It is very important to monitor their status so as to ensure that they operate efficiently and safely. Strain, temperature, and vibration are also required to be monitored.[156,157]

In the transportation industry, especially the aircraft industry, many manufacturers have started to use more composite materials to improve fuel efficiency and reduce emissions.[158] Composite materials, such as aluminum alloys, are lighter in weight but better in strength properties than conventional materials. Due to the complexity of composite materials, however, closer monitoring is required to avoid unpredictable behavior. Especially after excessive wing deformations caused in-flight destruction of NASA's space shuttle in 2003, the importance of such monitoring has been emphasized.[159] Thus, manufacturers have installed FBG sensors inside aircraft wings to closely monitor target materials. Nicolas et al. demonstrated the large-scale application of FBG sensors to an airplane. Specifically, they used more than 700 FBGs to determine the in-flight wing loads and shape. Fig. 21 shows the sensor locations on the wing surface.[159] Kang et al. studied thermal characteristics of FBG sensors at cryogenic temperatures for applying in the research fields concerning cryogenics such as space engineering and maglev systems in railway engineering.[160]

The optical fibers for SHM applications have been studied for monitoring of large infrastructures. However, most of OFS has
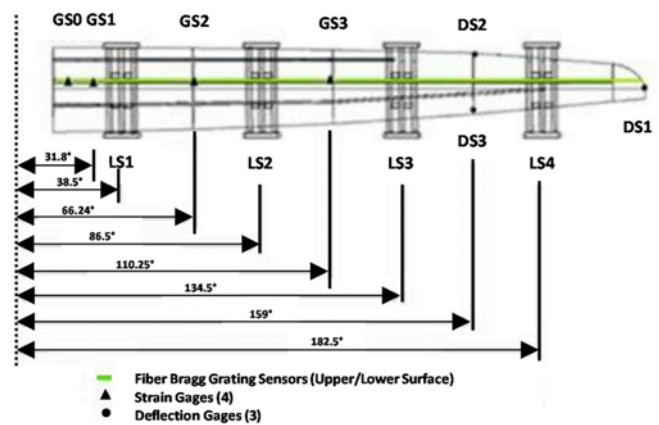

Fig. 21 FBG sensor locations on surface of wing structure[159] (Adapted from Ref. 159 with permission)

difficulty to decouple temperature and other properties like RI and strain. In order to solve this problem, it has been studied to decouple temperature and strain for various types of OFS such as FBG,[161] FPI,[162] Sagnac,[163] and Brillouin OTDA.[164] Moreover, fragility of bare fiber is a major concern in this field because the fiber sensor is easy to be damaged during the installation or measurement process. It has been improved by using distinctive coatings and protections for the optical fiber such as nylon, acrylate, polyimide coatings.[165]

4.3 OFS in Agricultural Engineering

In agricultural engineering, environmental monitoring sensors allow for understanding of the environmental impact of agricultural productivity. Farm conditions suitable for resources can be managed stably by environmental monitoring. In general, spectroscopic sensors are proposed for monitoring of the quality of air, soil, and water. Numerous studies have focused on the monitoring of farmland soil. Soil fertility is the main goal of farmers seeking to improve crop yields and productivity. In order to assist farmers' agronomic decisions, monitoring of changes in soil properties according to different farming methods is essential.

A portable sensor for soil monitoring is based on fiber-optic reflection spectroscopy (FORS). It consists of a light source, a spectrometer, and optical fiber bundles. The optical fibers are used to collect the reflected signals from the soil. It also enables long-distance transmission of optical signals at a high transmission rate and with low data loss. It thus makes possible the monitoring of soil properties across large temporal and spatial domains. FORS ranging 0.4 to 2.5 μm invisible-near infrared (Vis-NIR) is mainly used for soil monitoring.[166] An organic paddy field in Matsuyama City in Japan has been monitored by a customized Vis-NIR soil sensor. The soil sensor with optical fibers was attached to the tractor to monitor the soil properties in real-time while the tractor was traveling across the paddy field, as shown in Fig. 22(a).[30] A paddy field in Yongfeng village in Beijing in China was also investigated to understand the effects of water existence on the reflectance anisotropy of the canopy. A customized OF point sensor was used to monitor the reflected lights from the soft and muddy bottom of the paddy field for 10-15 days.[167] The flexibility of the OFS enables location of the sensing probe at any measurement point, even
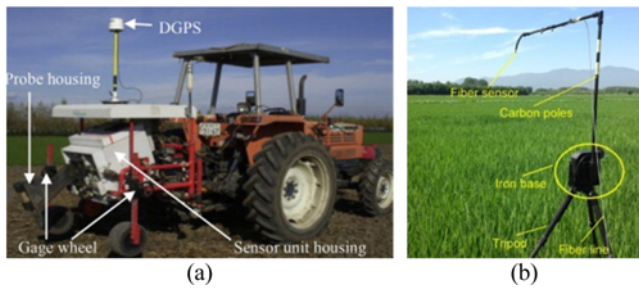
Fig. 22 Vis-NIR real-time soil sensors used in organic paddy field[30,167] (Adapted from Ref. 30 and 167 with permission)
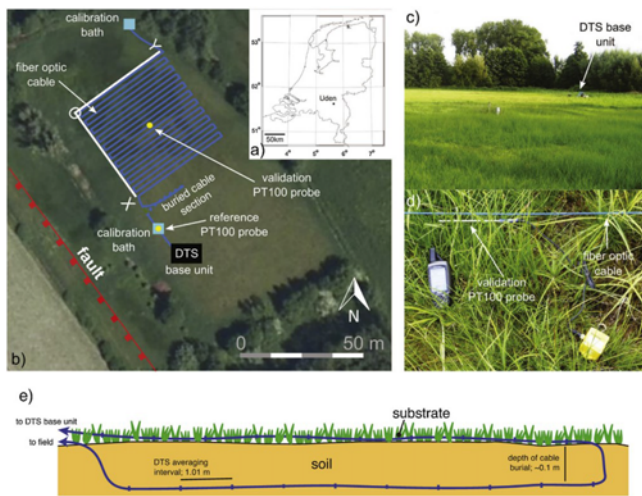

Fig. 23 Distributed sensing area for ground-temperature monitoring[171] (Adapted from Ref. 171 with permission)

in the air above the paddy field as shown in Fig. 22(b). It was found that the water background makes the reflectance anisotropy of the rice canopy weaken when the fraction of the vegetation cover is less than 80% or the depth of water is shallow less than 10cm. Soil from a coffee plantation in Brazil[168] and soil samples collected across the continental-scale transects of the USA[169] were analyzed by customized OFS for soil characterization. The customized OFS were applied in extreme environments such as tropical and subtropical soils.[170]

In the Netherlands, the distributed optical fiber sensor (DOFS) was proposed for temperature monitoring of a groundwater-fed wet meadow in the late summer season.[171] They observed that temperature fluctuations depend on the height of the canopy but that just after rainfall, temperature homogenizing occurred regardless of the height of the canopy, due specifically to water vaporization and radiation diffusion. Given that the fiber-optic distributed sensor has a configuration suitable for direct measurement of physical property distributions over a large area as shown in Fig. 23, it has been a promising analytical method for measurement of the properties of below-ground soil. Indeed, the distributed OFS can evaluate, real time, the spatial and temporal dynamics of the chemical[29] or physical[172] characteristics of the surface or of the underground.

Air monitoring by the spectrometric OFS has also been

investigated. In general, the concentrations of chemical gases are monitored to evaluate the atmospheric conditions for managing livestock or food. For example, in animal-feeding facilities, ammonia emissions from agricultural activities needs to be quantified for animal health management.[173] In New Zealand for instance, methane (CH_4) emissions from livestock constitute a large proportion, about 30%, of overall greenhouse gas emissions. Laubach et al. investigated the methane emissions from a herd of cattle in a paddock area of the Aorangi Research Farm located in the North Island of New Zealand.[174] Their proposed monitoring sensor was based on a Fourier-transform infra-red spectrometer and optical fiber bundles. Huang et al. proposed a bent OFS coated with BCP-doped solegel silica for ammonia (NH_3) monitoring in a real cattle feedlot.[175] The proposed sensor showed a sufficiently low detection limit enough for monitoring trace of NH_3. It has high selectivity and suffered no interference from the CO_2 concentration change. With those sensors' optical fiber cables as waveguides for measurement data, in situ monitoring of a large area was achieved. Moreover, the system was shown to be connectable to network systems at control sites.[176]

4.4 OFS Potentials in Manufacturing

As the interest in green technology has emerged and grown, process control in the environmental point of view has been required by the manufacturing industry. The OFS has the potential to monitor environmental properties under extreme manufacturing process such as drilling and turning. Monitoring of manufacturing conditions is crucial for eco-friendly and cost-effective process control. One engineering research group in Spain has proposed the use of a temperature sensor to monitor the workpiece temperature in the turning process.[177-179] A two-color fiber-optic pyrometer with the optical fibers was proposed to observe the localized areas. Mandal et al. studied a temperature sensor for scratching at micro-nano scale using FBG sensors. They measure the temperature changes at the tool tip under different scratching conditions like cutting speed.[180] The results showed the potential of the OFS to resolve problem presented by the difficulty of install any other sensors in cutting tools.

The monitoring of byproducts released into environments is crucial to management of the manufacturing process. Process control has to be achieved in order to minimize process residuals and wastes that, in most cases, cause environment pollution and present threats to humans. In the case of fossil-fuel power plants, real-time monitoring of unburned carbon in fly ash is required to evaluate combustion efficiency and its emission concentration.[181] Gaseous products, such as nitrite oxidases, carbon oxide, hydrocarbons, ammonia, oxygen, and hydrogen, among others,[182-184] are also required to be monitored in the manufacturing industry. Especially, CO_2 is a crucial analyte for environmental monitoring in a variety of manufacturing facilities ranging from fossil fuel power plants and underground geological sequestration to food production storage. Although many OFS designs for gas monitoring have been proposed to detect the specific concentrations of those gas species, interferometry-based OFS has complicated configurations. In the future more new types of OFS will be studied such as opto-acoustic,[185] optoelectronics,[186,187] and optofluidics.[188,189] Microstructured fiber also has great potentials as a platform for new types of OFS. For example, the hollow-core PCF with a single or arrays of air holes allows the manipulation of the

propagation of light and analytes resulting in high sensitivity.[190] Although the microstructured fibers can achieve high performance cost-effective manufacturing processes are also required for the commercialization of PCF-based sensors.[191]

5. Conclusions

The optical fiber sensor (OFS) has immunity to electromagnetic interferences and chemical corrosion, and is light weight, of small size, and boasts high flexibility; therefore, it can be effectively utilized for high sensitivity monitoring of chemical or physical properties in harsh, underground and subsea environments. In this paper, the OFS types employed for environmental monitoring in the fields of petroleum engineering, civil engineering, agricultural engineering, and manufacturing engineering were reviewed. Their respective principles were described according to the following classifications: point-based OFS and distributed OFS. Their fabrication processes, namely grating inscription, functional coating, and fiber shaping, also were detailed. Environmental monitoring applications have been investigated over the past five years. In the manufacturing point of view, the OFS has become a powerful tool of process control for improved energy efficiency and facility eco-friendliness.

ACKNOWLEDGEMENT

REFERENCES

1. Campbell, M. "Sensor Systems for Environmental Monitoring: Volume One: Sensor Technologies," Springer Science & Business Media, pp. 1-36, 2012.

2. Ho, C. K., Robinson, A., Miller, D. R., and Davis, M. J., "Overview of Sensors and Needs for Environmental Monitoring," Sensors, Vol. 5, No. 1, pp. 4-37, 2005.

3. Harrison, R. M. "Understanding our Environment: An Introduction to Environmental Chemistry and Pollution," Royal Society of Chemistry, 2007.

4. Timmer, B., Olthuis, W., and Van den Berg, A., "Ammonia Sensors and their Applications—A Review," Sensors and Actuators B: Chemical, Vol. 107, No. 2, pp. 666-677, 2005.

5. Korotcenkov, G., Han, S. D., and Stetter, J. R., "Review of Electrochemical Hydrogen Sensors," Chemical Reviews, Vol. 109, No. 3, pp. 1402-1433, 2009.

6. Shuk, P. and Jantz, R., "Oxygen Gas Sensing Technologies: A Comprehensive Review," Proc. of the 9th International Conference on Sensing Technology, pp. 12-17, 2015.

7. Rheaume, J. M. and Pisano, A. P., "A Review of Recent Progress in Sensing of Gas Concentration by Impedance Change," Ionics, Vol. 17, No. 2, pp. 99-108, 2011.

8. Korotcenkov, G., Brinzari, V., and Cho, B. K., "Conductometric Gas Sensors Based on Metal Oxides Modified with Gold Nanoparticles: A Review," Microchimica Acta, Vol. 183, No. 3, pp. 1033-1054, 2016.

9. Jiang, G., Goledzinowski, M., Comeau, F. J., Zarrin, H., Lui, G., et al., "Free-Standing Functionalized Graphene Oxide Solid Electrolytes in Electrochemical Gas Sensors," Advanced Functional Materials, Vol. 26, No. 11, pp. 1729-1736, 2016.

10. Stetter, J. R. and Li, J., "Amperometric Gas Sensors A Review," Chemical Reviews, Vol. 108, No. 2, pp. 352-366, 2008.

11. Mead, M., Popoola, O., Stewart, G., Landshoff, P., Calleja, M., et al., "The Use of Electrochemical Sensors for Monitoring Urban Air Quality in Low-Cost, High-Density Networks," Atmospheric Environment, Vol. 70, pp. 186-203, 2013.

12. Swallow, J. G., Kim, J. J., Maloney, J. M., Chen, D., Smith, J. F., et al., "Dynamic Chemical Expansion of Thin-Film Non-Stoichiometric Oxides at Extreme Temperatures," Nature Materials, Vol. 16, No. 7, pp. 749-754, 2017.

13. Jiang, X., Kim, K., Zhang, S., Johnson, J., and Salazar, G., "High-Temperature Piezoelectric Sensing," Sensors, Vol. 14, No. 1, pp. 144-169, 2013.

14. Moos, R., Izu, N., Rettig, F., Reiß, S., Shin, W., et al., "Resistive Oxygen Gas Sensors for Harsh Environments," Sensors, Vol. 11, No. 4, pp. 3439-3465, 2011.

15. Erfan, M., Sabry, Y. M., Sakr, M., Mortada, B., Medhat, M., et al., "On-Chip Micro–Electro–Mechanical System Fourier Transform Infrared (MEMS FT-IR) Spectrometer-Based Gas Sensing," Applied Spectroscopy, Vol. 70, No. 5, pp. 897-904, 2016.

16. Ciuti, G., Ricotti, L., Menciassi, A., and Dario, P., "Mems Sensor Technologies for Human Centred Applications in Healthcare, Physical Activities, Safety and Environmental Sensing: A Review on Research Activities in Italy," Sensors, Vol. 15, No. 3, pp. 6441-6468, 2015.

17. Tong, X. C., "Advanced Materials and Design for Electromagnetic Interference Shielding," CRC press, pp. 2-3, 2016.

18. Keiser, G., "Optical Fiber Communications," John Wiley & Sons, 2003.

19. Frieden, R., "Managing Internet-Driven Change in International Telecommunications," Artech House, 2001.

20. Submarine Cable Map, https://www.submarinecablemap.com/. (Accessed 22 DEC 2017)

21. Fang, Z., Chin, K., Qu, R., and Cai, H., "Fundamentals of Optical Fiber Sensors," John Wiley & Sons, 2012.

22. Huang, J.-Y., Van Roosbroeck, J., Martinez, A. B., Geernaert, T., Berghmans, F., et al., "Fiber Bragg Grating Sensors Written by

Femtosecond Laser Pulses in Micro-Structured Fiber for Downhole Pressure Monitoring," Proc. of Optical Fiber Sensors Conference, pp. 1-4, 2017.

23. Li, J., Liao, K., Kong, X., Li, S., Zhang, X., et al., "Nuclear Power Plant Prestressed Concrete Containment Vessel Structure Monitoring during integrated Leakage Rate Testing Using Fiber Bragg Grating Sensors," Applied Sciences, Vol. 7, No. 4, Article No. 419, 2017.

24. Perez-Herrera, R. and Lopez-Amo, M., "Fiber Optic Sensor Networks," Optical Fiber Technology, Vol. 19, No. 6, pp. 689-699, 2013.

25. Madabhushi, S., Elshafie, M., and Haigh, S. K., "Accuracy of Distributed Optical Fiber Temperature Sensing for Use in Leak Detection of Subsea Pipelines," Journal of Pipeline Systems Engineering and Practice, Vol. 6, No. 2, Paper No. 04014014, 2014.

26. Kobs, S., Holland, D. M., Zagorodnov, V., Stern, A., and Tyler, S. W., "Novel Monitoring of Antarctic Ice Shelf Basal Melting Using a Fiber-Optic Distributed Temperature Sensing Mooring," Geophysical Research Letters, Vol. 41, No. 19, pp. 6779-6786, 2014.

27. Pei, H., Cui, P., Yin, J., Zhu, H., Chen, X., et al., "Monitoring and Warning of Landslides and Debris Flows Using an Optical Fiber Sensor Technology," Journal of Mountain Science, Vol. 8, No. 5, p. 728, 2011.

28. Jaroszewicz, L., Krajewski, Z., Solarz, L., and Teisseyer, R., "Application of the Fibre-Optic Sagnac Interferometer in the Investigation of Seismic Rotational Waves," Measurement Science and Technology, Vol. 17, No. 5, p. 1186, 2006.

29. Cao, D., Shi, B., Zhu, H., Wei, G., Chen, S.-E., et al., "A Distributed Measurement Method for In-Situ Soil Moisture Content by Using Carbon-Fiber Heated Cable," Journal of Rock Mechanics and Geotechnical Engineering, Vol. 7, No. 6, pp. 700-707, 2015.

30. Baharom, S. N. A., Shibusawa, S., Kodaira, M., and Kanda, R., "Multiple-Depth Mapping of Soil Properties Using a Visible and Near Infrared Real-Time Soil Sensor for a Paddy Field," Engineering in Agriculture, Environment and Food, Vol. 8, No. 1, pp. 13-17, 2015.

31. Hill, K., Fujii, Y., Johnson, D. C., and Kawasaki, B., "Photosensitivity in Optical Fiber Waveguides: Application to Reflection Filter Fabrication," Applied Physics Letters, Vol. 32, No. 10, pp. 647-649, 1978.

32. Othonos, A., "Fiber Bragg Gratings," Review of Scientific Instruments, Vol. 68, No. 12, pp. 4309-4341, 1997.

33. Kalachev, A. I., Pureur, V., and Nikogosyan, D. N., "Investigation of Long-Period Fiber Gratings Induced by High-Intensity Femtosecond UV Laser Pulses," Optics Communications, Vol. 246, No. 1, pp. 107-115, 2005.

34. Wang, Y., "Review of Long Period Fiber Gratings Written by CO_2 Laser," Journal of Applied Physics, Vol. 108, No. 8, p. 11, 2010.

35. Fujimaki, M., Ohki, Y., Brebner, J. L., and Roorda, S., "Fabrication of Long-Period Optical Fiber Gratings by Use of Ion Implantation," Optics Letters, Vol. 25, No. 2, pp. 88-89, 2000.

36. Palai, P., Satyanarayan, M., Das, M., Thyagarajan, K., and Pal, B., "Characterization and Simulation of Long Period Gratings Fabricated Using Electric Discharge," Optics Communications, Vol. 193, No. 1, pp. 181-185, 2001.

37. Lin, C.-Y., Chern, G.-W., and Wang, L. A., "Periodical Corrugated Structure for Forming Sampled Fiber Bragg Grating and Long-Period Fiber Grating with Tunable Coupling Strength," Journal of Lightwave Technology, Vol. 19, No. 8, p. 1212, 2001.

38. Savin, S., Digonnet, M., Kino, G., and Shaw, H., "Tunable Mechanically Induced Long-Period Fiber Gratings," Optics Letters, Vol. 25, No. 10, pp. 710-712, 2000.

39. Kashyap, R., "Fiber Bragg Gratings," Academic Press, p. 480, 2009.

40. Cusano, A., Cutolo, A., and Albert, J., "Fiber Bragg Grating Sensors: Recent Advancements, Industrial Applications and Market Exploitation," Bentham Science Publishers, 2011.

41. Kinet, D., Mégret, P., Goossen, K. W., Qiu, L., Heider, D., et al., "Fiber Bragg Grating Sensors Toward Structural Health Monitoring in Composite Materials: Challenges and Solutions," Sensors, Vol. 14, No. 4, pp. 7394-7419, 2014.

42. Bhatia, V. and Vengsarkar, A. M., "Optical Fiber Long-Period Grating Sensors," Optics Letters, Vol. 21, No. 9, pp. 692-694, 1996.

43. Vengsarkar, A. M., Lemaire, P. J., Judkins, J. B., Bhatia, V., Erdogan, T., et al., "Long-Period Fiber Gratings as Band-Rejection Filters," Journal of Lightwave Technology, Vol. 14, No. 1, pp. 58-65, 1996.

44. Patrick, H., Chang, C., and Vohra, S., "Long Period Fibre Gratings for Structural Bend Sensing," Electronics Letters, Vol. 34, No. 18, pp. 1773-1775, 1998.

45. Li, L., Xia, L., Xie, Z., and Liu, D., "All-Fiber Mach-Zehnder Interferometers for Sensing Applications," Optics Express, Vol. 20, No. 10, pp. 11109-11120, 2012.

46. Fu, H., Zhao, N., Shao, M., Li, H., Gao, H., et al., "High-Sensitivity Mach–Zehnder Interferometric Curvature Fiber Sensor Based on Thin-Core Fiber," IEEE Sensors Journal, Vol. 15, No. 1, pp. 520-525, 2015.

47. Harris, J., Lu, P., Larocque, H., Chen, L., and Bao, X., "In-Fiber Mach–Zehnder Interferometric Refractive Index Sensors with Guided and Leaky Modes," Sensors and Actuators B: Chemical, Vol. 206, pp. 246-251, 2015.

48. Lee, B. H., Kim, Y. H., Park, K. S., Eom, J. B., Kim, M. J., et al., "Interferometric Fiber Optic Sensors," Sensors, Vol. 12, No. 3, pp. 2467-2486, 2012.

49. Hong, S., Jung, W., Nazari, T., Song, S., Kim, T., et al., "Thermo-Optic Characteristic of DNA Thin Solid Film and Its Application as a Biocompatible Optical Fiber Temperature Sensor," Optics Letters, Vol. 42, No. 10, pp. 1943-1945, 2017.

50. Zhang, S., Dong, X., Li, T., Chan, C. C., and Shum, P. P., "Simultaneous Measurement of Relative Humidity and Temperature with PCF-MZI Cascaded by Fiber Bragg Grating," Optics Communications, Vol. 303, pp. 42-45, 2013.

51. Liu, Y., Li, Y., Yan, X., and Li, W., "Effect of Waist Diameter and Twist on Tapered Asymmetrical Dual-Core Fiber MZI Filter," Applied Optics, Vol. 54, No. 28, pp. 8248-8253, 2015.

52. Zhu, T., Wu, D., Liu, M., and Duan, D.-W., "In-Line Fiber Optic Interferometric Sensors in Single-Mode Fibers," Sensors, Vol. 12, No. 8, pp. 10430-10449, 2012.

53. Kashyap, R. and Nayar, B., "An All Single-Mode Fiber Michelson Interferometer Sensor," Journal of Lightwave Technology, Vol. 1, No. 4, pp. 619-624, 1983.

54. Bahrampour, A. R., Tofighi, S., Bathaee, M., and Farman, F., "Optical Fiber Interferometers and their Applications," Interferometry-Research and Applications in Science and Technology, 2012.

55. Swart, P. L., "Long-Period Grating Michelson Refractometric Sensor," Measurement Science and Technology, Vol. 15, No. 8, p. 1576, 2004.

56. Hu, P., Dong, X., Ni, K., Chen, L. H., Wong, W. C., et al., "Sensitivity-Enhanced Michelson Interferometric Humidity Sensor with Waist-Enlarged Fiber Bitaper," Sensors and Actuators B: Chemical, Vol. 194, pp. 180-184, 2014.

57. Yoshino, T., Kurosawa, K., Itoh, K., and Ose, T., "Fiber-Optic Fabry-Perot Interferometer and Its Sensor Applications," IEEE Transactions on Microwave Theory and Techniques, Vol. 30, No. 10, pp. 1612-1621, 1982.

58. Duraibabu, D. B., Poeggel, S., Omerdic, E., Capocci, R., Lewis, E., et al., "An Optical Fibre Depth (Pressure) Sensor for Remote Operated Vehicles in Underwater Applications," Sensors, Vol. 17, No. 2, pp. 406-418, 2017.

59. Islam, M. R., Ali, M. M., Lai, M.-H., Lim, K.-S., and Ahmad, H., "Chronology of Fabry-Perot Interferometer Fiber-Optic Sensors and their Applications: A Review," Sensors, Vol. 14, No. 4, pp. 7451-7488, 2014.

60. Zhu, Y. and Wang, A., "Miniature Fiber-Optic Pressure Sensor," IEEE Photonics Technology Letters, Vol. 17, No. 2, pp. 447-449, 2005.

61. Culshaw, B., "The Optical Fibre Sagnac Interferometer: An Overview of Its Principles and Applications," Measurement Science and Technology, Vol. 17, No. 1, pp. R1-R16, 2005.

62. Kurzych, A., Jaroszewicz, L. R., Krajewski, Z., Teisseyre, K. P., and Kowalski, J. K., "Fibre Optic System for Monitoring Rotational Seismic Phenomena," Sensors, Vol. 14, No. 3, pp. 5459-5469, 2014.

63. Jaroszewicz, L. R., Kurzych, A., Krajewski, Z., Marć, P., Kowalski, J. K., et al., "Review of the Usefulness of Various Rotational Seismometers with Laboratory Results of Fibre-Optic Ones Tested for Engineering Applications," Sensors, Vol. 16, No. 12, pp. 2161, 2016.

64. Hartog, A. H., "An Introduction to Distributed Optical Fibre Sensors," CRC Press, 2017.

65. Kingsley, S. and Davies, D., "OFDR Diagnostics for Fibre and Integrated-Optic Systems," Electronics Letters, Vol. 21, No. 10, pp. 434-435, 1985.

66. Mukhopadhyay, S. C., "New Developments in Sensing Technology for Structural Health Monitoring," Springer Berlin Heidelberg, 2011.

67. Barrias, A., Casas, J. R., and Villalba, S., "A Review of Distributed Optical Fiber Sensors for Civil Engineering Applications," Sensors, Vol. 16, No. 5, p. 748, 2016.

68. Froggatt, M. and Moore, J., "High-Spatial-Resolution Distributed Strain Measurement in Optical Fiber with Rayleigh Scatter," Applied Optics, Vol. 37, No. 10, pp. 1735-1740, 1998.

69. Eun, K., Lee, K. J., Lee, K. K., Yang, S. S., and Choa, S.-H., "Highly Sensitive Surface Acoustic Wave Strain Sensor for the Measurement of Tire Deformation," Int. J. Precis. Eng. Manuf., Vol. 17, No. 6, pp. 699-707, 2016.

70. Mateeva, A., Lopez, J., Potters, H., Mestayer, J., Cox, B., et al., "Distributed Acoustic Sensing for Reservoir Monitoring with Vertical Seismic Profiling," Geophysical Prospecting, Vol. 62, No. 4, pp. 679-692, 2014.

71. Galindez-Jamioy, C. A. and Lopez-Higuera, J. M., "Brillouin Distributed Fiber Sensors: An Overview and Applications," Journal of Sensors, 2012.

72. Yeniay, A., Delavaux, J.-M., and Toulouse, J., "Spontaneous and Stimulated Brillouin Scattering Gain Spectra in Optical Fibers," Journal of Lightwave Technology, Vol. 20, No. 8, pp. 1425, 2002.

73. Lim, K., Wong, L., Chiu, W. K., and Kodikara, J., "Distributed Fiber Optic Sensors for Monitoring Pressure and Stiffness Changes in Out-of-Round Pipes," Structural Control and Health Monitoring, Vol. 23, No. 2, pp. 303-314, 2016.

74. Maraval, D., Gabet, R., Jaouen, Y., and Lamour, V., "Dynamic Optical Fiber Sensing with Brillouin Optical Time Domain Reflectometry: Application to Pipeline Vibration Monitoring," Journal of Lightwave Technology, Vol. 35, No. 16, pp. 3296-3302, 2017.

75. Long, D. A., "The Raman Effect: A Unified Treatment of the Theory of Raman Scattering by Molecules," West Sussex, 2002.

76. Pandian, C., Kasinathan, M., Sosamma, S., Rao, C. B., Jayakumar, T., et al., "Raman Distributed Sensor System for Temperature Monitoring and Leak Detection in Sodium Circuits of FBR," Proc. of 1st International Conference on Advancements in Nuclear Instrumentation Measurement Methods and their Applications, pp. 1-4, 2009.

77. Lee, C.-M., Woo, W.-S., Kim, D.-H., Oh, W.-J., and Oh, N.-S., "Laser-Assisted Hybrid Processes: A Review," Int. J. Precis. Eng. Manuf., Vol. 17, No. 2, pp. 257-267, 2016.

78. Lee, H., Lim, C. H. J., Low, M. J., Tham, N., Murukeshan, V. M., et al., "Lasers in Additive Manufacturing: A Review," Int. J. Precis. Eng. Manuf.-Green Tech., Vol. 4, No. 3, pp. 307-322, 2017.

79. Mihailov, S. J., "Fiber Bragg Grating Sensors for Harsh Environments," Sensors, Vol. 12, No. 2, pp. 1898-1918, 2012.

80. Martinez, A., Dubov, M., Khrushchev, I., and Bennion, I., "Direct Writing of Fibre Bragg Gratings by Femtosecond Laser," Electronics Letters, Vol. 40, No. 19, pp. 1170-1172, 2004.

81. Gattass, R. R. and Mazur, E., "Femtosecond Laser Micromachining in Transparent Materials," Nature Photonics, Vol. 2, No. 4, pp. 219-225, 2008.

82. Meltz, G., Morey, W. W., and Glenn, W., "Formation of Bragg Gratings in Optical Fibers by a Transverse Holographic Method," Optics Letters, Vol. 14, No. 15, pp. 823-825, 1989.

83. Loh, W., Cole, M., Zervas, M. N., Barcelos, S., and Laming, R., "Complex Grating Structures with Uniform Phase Masks Based on the Moving Fiber–Scanning Beam Technique," Optics Letters, Vol. 20, No. 20, pp. 2051-2053, 1995.

84. Ahmed, F., Joe, H.-E., Min, B.-K., and Jun, M. B., "Characterization of Refractive Index Change and Fabrication of Long Period Gratings in Pure Silica Fiber by Femtosecond Laser Radiation," Optics & Laser Technology, Vol. 74, pp. 119-124, 2015.

85. Yong, Z., Zhan, C., Lee, J., Yin, S., and Ruffin, P., "Multiple Parameter Vector Bending and High-Temperature Sensors Based on Asymmetric Multimode Fiber Bragg Gratings Inscribed by an Infrared Femtosecond Laser," Optics Letters, Vol. 31, No. 12, pp. 1794-1796, 2006.

86. Dostovalov, A. V., Wolf, A. A. E., and Babin, S. A., "Long-Period Fibre Grating Writing with a Slit-Apertured Femtosecond Laser Beam ($\lambda = 1026$ nm)," Quantum Electronics, Vol. 45, No. 3, pp. 235, 2015.

87. Melo, L., Burton, G., Warwick, S., and Wild, P. M., "Experimental Investigation of Long-Period Grating Transition Modes to Monitor CO_2 in High-Pressure Aqueous Solutions," Journal of Lightwave Technology, Vol. 33, No. 12, pp. 2554-2560, 2015.

88. Zhang, Y.-N., Peng, H., Qian, X., Zhang, Y., An, G., et al., "Recent Advancements in Optical Fiber Hydrogen Sensors," Sensors and Actuators B: Chemical, Vol. 244, pp. 393-416, 2017.

89. Xie, W., Yang, M., Cheng, Y., Li, D., Zhang, Y., et al., "Optical Fiber Relative-Humidity Sensor with Evaporated Dielectric Coatings on Fiber End-Face," Optical Fiber Technology, Vol. 20, No. 4, pp. 314-319, 2014.

90. Ghadiry, M., Gholami, M., Choon Kong, L., Wu Yi, C., Ahmad, H., et al., "Nano-Anatase TiO_2 for High Performance Optical Humidity Sensing on Chip," Sensors, Vol. 16, No. 1, pp. 39, 2015.

91. Richter, A., Paschew, G., Klatt, S., Lienig, J., Arndt, K.-F., et al., "Review on Hydrogel-Based pH Sensors and Microsensors," Sensors, Vol. 8, No. 1, pp. 561-581, 2008.

92. Yan, M., Tylczak, J., Yu, Y., Panagakos, G., and Ohodnicki, P., "Multi-Component Optical Sensing of High Temperature Gas Streams Using Functional Oxide Integrated Silica Based Optical Fiber Sensors," Sensors and Actuators B: Chemical, Vol. 255, pp. 357-365, 2018.

93. Fu, H., Jiang, Y., Ding, J., Zhang, J., Zhang, M., et al., "Zinc Oxide Nanoparticle Incorporated Graphene Oxide as Sensing Coating for Interferometric Optical Microfiber for Ammonia Gas Detection," Sensors and Actuators B: Chemical, Vol. 254, pp. 239-247, 2017.

94. Yu, C., Wu, Y., Liu, X., Fu, F., Gong, Y., et al., "Miniature Fiber-Optic NH3 Gas Sensor Based on Pt Nanoparticle-Incorporated Graphene Oxide," Sensors and Actuators B: Chemical, Vol. 244, pp. 107-113, 2017.

95. Matias, I. R., Ikezawa, S., and Corres, J., "Fiber Optic Sensors: Current Status and Future Possibilities," Springer, 2016.

96. Dominik, M., Koba, M., Bogdanowicz, R., Bock, W., and Śmietana, M., "Plasma-Based Deposition and Processing Techniques for Optical Fiber Sensing," in: Fiber Optic Sensors, Matian, I. R., Ikezawa, S., and Corres, J., (Eds.), Springer, pp. 95-114, 2017.

97. Yang, M., Peng, J., Wang, G., and Dai, J., "Fiber Optic Sensors Based on Nano-Films," in: Fiber Optic Sensors, Matian, I. R., Ikezawa, S., and Corres, J., (Eds.), Springer, pp. 1-30, 2017.

98. Seshan, K., "Handbook of Thin Film Deposition," William Andrew, 2012.

99. Ficek, M., Drijkoningen, S., Karczewski, J., Bogdanowicz, R., and Haenen, K., "Low Temperature Growth of Diamond Films on Optical Fibers Using Linear Antenna CVD System," Proc. of IOP Conference Series: Materials Science and Engineering, Paper No. 012025, 2016.

100. Majchrowicz, D., Hirsch, M., Wierzba, P., Bechelany, M., Viter, R., et al., "Application of Thin ZnO ALD Layers in Fiber-Optic Fabry-Pérot Sensing Interferometers," Sensors, Vol. 16, No. 3, pp. 416, 2016.

101. Melo, L., Burton, G., Kubik, P., and Wild, P., "Refractive Index Sensor Based on Inline Mach-Zehnder Interferometer Coated with Hafnium Oxide by Atomic Layer Deposition," Sensors and Actuators B: Chemical, Vol. 236, pp. 537-545, 2016.

102. Volkert, C. A. and Minor, A. M., "Focused Ion Beam Microscopy and Micromachining," MRS Bulletin, Vol. 32, No. 5, pp. 389-399, 2007.

103. André, R. M., Pevec, S., Becker, M., Dellith, J., Rothhardt, M., et al., "Focused Ion Beam Post-Processing of Optical Fiber Fabry-Perot Cavities for Sensing Applications," Optics Express, Vol. 22, No. 11, pp. 13102-13108, 2014.

104. Kou, J.-L., Qiu, S.-J., Xu, F., Lu, Y.-Q., Yuan, Y., et al., "Miniaturized Metal-Dielectric-Hybrid Fiber Tip Grating for Refractive Index Sensing," IEEE Photonics Technology Letters, Vol. 23, No. 22, pp. 1712-1714, 2011.

105. Ahmed, F., Ahsani, V., Melo, L., Wild, P., and Jun, M. B., "Miniaturized Tapered Photonic Crystal Fiber Mach–Zehnder Interferometer for Enhanced Refractive Index Sensing," IEEE Sensors Journal, Vol. 16, No. 24, pp. 8761-8766, 2016.

106. Tseng, S.-M. and Chen, C.-L., "Side-Polished Fibers," Applied Optics, Vol. 31, No. 18, pp. 3438-3447, 1992.

107. Gaston, A., Lozano, I., Perez, F., Auza, F., and Sevilla, J., "Evanescent Wave Optical-Fiber Sensing (Temperature, Relative Humidity, and pH Sensors)," IEEE Sensors Journal, Vol. 3, No. 6, pp. 806-811, 2003.

108. Wei, H., Zhu, Y., and Krishnaswamy, S., "Optofluidic Photonic Crystal Fiber Coupler for Measuring the Refractive Index of Liquids," IEEE Photonics Technology Letters, Vol. 28, No. 1, pp. 103-106, 2016.

109. Borzycki, K. and Schuster, K., "Arc Fusion Splicing of Photonic Crystal Fibres," Photonic Crystals-Introduction, Applications and Theory, 2012.

110. Chong, J. H., Rao, M., Zhu, Y., and Shum, P., "An Effective Splicing Method on Photonic Crystal Fiber Using CO_2 Laser," IEEE Photonics Technology Letters, Vol. 15, No. 7, pp. 942-944, 2003.

111. Qiao, X., Shao, Z., Bao, W., and Rong, Q., "Fiber Bragg Grating Sensors for the Oil Industry," Sensors, Vol. 17, No. 3, p. 429, 2017.

112. Bao, X. and Chen, L., "Recent Progress in Distributed Fiber Optic Sensors," Sensors, Vol. 12, No. 7, pp. 8601-8639, 2012.

113. Gyger, F., Chin, S., Rochat, E., Ravet, F., and Niklès, M., "Ultra Long Range DTS (> 300 km) to Support Deep Offshore and Long Tieback Developments," Proc. of 33rd International Conference on Ocean, Offshore and Arctic Engineering, in American Society of Mechanical Engineers, pp. V06BT04A001-V006BT004A001, 2014.

114. Ravet, F., Rochat, E., and Niklès, M., "Challenges, Requirements and Advances for Distributed Fiber Optic Sensors in Surf Structures and Subsea Well Monitoring," Proc. of American Society of Mechanical Engineers, 2013.

115. Lin, W. T., Lou, S. Q., and Liang, S., "Fiber-Optic Distributed Vibration Sensor for Pipeline Pre-Alarm," Proc. of the Applied Mechanics and Materials, pp. 235-239, 2014.

116. Worsley, J., Minto, C., Hill, D., Godfrey, A., and Ashdown, J., "Fibre Optic Four Mode Leak Detection for Gas, Liquids and Multiphase Products," Proc. of Abu Dhabi International Petroleum Exhibition and Conference, pp. 10-13, 2014.

117. Varela, F., Yongjun Tan, M., and Forsyth, M., "An Overview of Major Methods for Inspecting and Monitoring External Corrosion of On-Shore Transportation Pipelines," Corrosion Engineering, Science and Technology, Vol. 50, No. 3, pp. 226-235, 2015.

118. Pnev, A., Zhirnov, A., Stepanov, K., Nesterov, E., Shelestov, D., et al., "Mathematical Analysis of Marine Pipeline Leakage Monitoring System Based on Coherent OTDR with Improved Sensor Length and Sampling Frequency," Journal of Physics: Conference Series, Paper No. 012016, 2015.

119. Wong, L., Rathnayaka, S., Chiu, W., and Kodikara, J., "Fatigue Damage Monitoring of a Cast Iron Pipeline Using Distributed Optical Fibre Sensors," Procedia Engineering, Vol. 188, pp. 293-300, 2017.

120. Mirzaei, A., Bahrampour, A., Taraz, M., Bahrampour, A., Bahrampour, M., et al., "Transient Response of Buried Oil Pipelines Fiber Optic Leak Detector Based on the Distributed Temperature Measurement," International Journal of Heat and Mass Transfer, Vol. 65, pp. 110-122, 2013.

121. Jin, B., Wang, Y., Wang, Y., and Wang, D., "Application Research of Distributed Optical Fiber Sensing Technology Used in Safety Monitoring of Coalbed Methane Pipelines," Proc. of the Progress in Electromagnetic Research Symposium, pp. 4903-4906, 2016.

122. Jiang, T., Ren, L., Jia, Z. G., Li, D. S., and Li, H. N., "Pipeline Internal Corrosion Monitoring Based on Distributed Strain Measurement Technique," Structural Control and Health Monitoring, 2017.

123. Wang, F., Sun, Z., Zhu, F., Zhu, C., Pan, Y., et al., "Research on the Leakage Monitoring of Oil Pipeline Using BOTDR," Proc. of Progress in Electromagnetic Research Symposium, pp. 4907-4910, 2016.

124. Peng, F., Wu, H., Jia, X.-H., Rao, Y.-J., Wang, Z.-N., et al., "Ultra-Long High-Sensitivity φ-OTDR for High Spatial Resolution Intrusion Detection of Pipelines," Optics Express, Vol. 22, No. 11, pp. 13804-13810, 2014.

125. Tan, D., Tian, X., Sun, W., Zhou, Y., Liu, L., et al., "An Oil & Gas Pipeline Pre-Warning System Based on φ-OTDR," Proc. of the 23rd International Conference on Optical Fiber Sensors, Paper No. 91578W, 2014.

126. Tejedor, J., Macias-Guarasa, J., Martins, H. F., Piote, D., Pastor-Graells, J., et al., "A Novel Fiber Optic Based Surveillance System for Prevention of Pipeline Integrity Threats," Sensors, Vol. 17, No. 2, pp. 355, 2017.

127. Wang, J., Zhao, L., Liu, T., Li, Z., Sun, T., et al., "Novel Negative Pressure Wave-Based Pipeline Leak Detection System Using Fiber Bragg Grating-Based Pressure Sensors," Journal of Lightwave Technology, Vol. 35, No. 16, pp. 3366-3373, 2017.

128. Freire, J., Perrut, V., Braga, A., Vieira, R., Ribeiro, A., et al., "Use of FBG Strain Gages on a Pipeline Specimen Repaired with a CFRE Composite," Experimental Techniques, Vol. 39, No. 5, pp. 70-79, 2015.

129. Hou, Q., Ren, L., Jiao, W., Zou, P., and Song, G., "An Improved Negative Pressure Wave Method for Natural Gas Pipeline Leak Location Using FBG Based Strain Sensor and Wavelet Transform," Mathematical Problems in Engineering, 2013.

130. Hou, Q., Jiao, W., Ren, L., Cao, H., and Song, G., "Experimental Study of Leakage Detection of Natural Gas Pipeline Using FBG Based Strain Sensor and Least Square Support Vector Machine," Journal of Loss Prevention in the Process Industries, Vol. 32, pp. 144-151, 2014.

131. Ren, L., Jia, Z., Ho, M. S. C., Yi, T., and Li, H., "Application of Fiber Bragg Grating Based Strain Sensor in Pipeline Vortex-Induced Vibration Measurement," Science China Technological Sciences, Vol. 57, No. 9, pp. 1714-1720, 2014.

132. Jiang, T., Ren, L., Jia, Z., Li, D., and Li, H., "Application of FBG Based Sensor in Pipeline Safety Monitoring," Applied Sciences, Vol. 7, No. 6, pp. 1-12, 2017.

133. Ríos, J. D. B., Torres, C. E., Aristizabal, J. H., Galvis, A., Díaz, R. A., et al., "Monitoring Stress/Strain in Buried Pipelines Through the Use of Fiber Bragg Grating Sensors," International Pipeline Geotechnical Conference in American Society of Mechanical Engineers, pp. V001T003A007-V001T003A007, 2015.

134. Felli, F., Paolozzi, A., Vendittozzi, C., Paris, C., and Asanuma, H., "Use of FBG Sensors for Health Monitoring of Pipelines," Proc. of the International Society for Optics and Photonics in Sensors and Smart Structures Technologies for Civil, Mechanical, and Aerospace System, Paper No. 98031L, 2016.

135. Cuéllar-Franca, R. M. and Azapagic, A., "Carbon Capture, Storage and Utilisation Technologies: A Critical Analysis and Comparison of their Life Cycle Environmental Impacts," Journal of CO_2 Utilization, Vol. 9, pp. 82-102, 2015.

136. Bao, B., Melo, L., Davies, B., Fadaei, H., Sinton, D., et al., "Detecting Supercritical CO_2 in Brine at Sequestration Pressure with an Optical Fiber Sensor," Environmental Science & Technology, Vol. 47, No. 1, pp. 306-313, 2012.

137. Li, Y., Zhu, W., Cheng, B., Nygaard, R., and Xiao, H., "Laboratory Evaluation of Distributed Coaxial Cable Temperature Sensors for Application in CO_2 Sequestration Well Characterization," Greenhouse Gases: Science and Technology, Vol. 6, No. 6, pp. 812-823, 2016.

138. Feng, X., Wu, W., Meng, D., Ansari, F., and Zhou, J., "Distributed Monitoring Method for Upheaval Buckling in Subsea Pipelines with Brillouin Optical Time-Domain Analysis Sensors," Advances in Structural Engineering, Vol. 20, No. 2, pp. 180-190, 2017.

139. Seaman, C. H., Brower, D. V., Le, S. Q., and Tang, H. H., "Development and Testing of a Post-Installable Deepwater Monitoring System Using Fiber-Optic Sensors," Proc. of the 34th International Conference on Ocean, Offshore, and Arctic Engineering, Paper No. V05BT04A048, 2015.

140. Bentley, N. L., Brower, D. V., Le, S. Q., Seaman, C. H., and Tang, H. H., "Development and Testing of a Friction-Based Post-Installable Sensor for Subsea Fiber-Optic Monitoring System," Proc. of the 36th International Conference on Ocean, Arctic Engineering, 2017.

141. Razali, N., Bakar, M. A., Tamchek, N., Yaacob, M., Latif, A., et al., "Fiber Bragg Grating for Pressure Monitoring of Full Composite Lightweight Epoxy Sleeve Strengthening System for Submarine Pipeline," Journal of Natural Gas Science and Engineering, Vol. 26, pp. 135-141, 2015.

142. Xu, J., Yang, D., Qin, C., Jiang, Y., Sheng, L., et al., "Study and Test of a New Bundle-Structure Riser Stress Monitoring Sensor Based on FBG," Sensors, Vol. 15, No. 11, pp. 29648-29660, 2015.

143. Hwang, D., Yoon, D.-J., Kwon, I.-B., Seo, D.-C., and Chung, Y., "Novel Auto-Correction Method in a Fiber-Optic Distributed-Temperature Sensor Using Reflected Anti-Stokes Raman Scattering," Optics Express, Vol. 18, No. 10, pp. 9747-9754, 2010.

144. Yamate, T., Fujisawa, G., and Ikegami, T., "Optical Sensors for the Exploration of Oil and Gas," Journal of Lightwave Technology, Vol. 35, No. 16, pp. 3538-3545, 2017.

145. Sanders, P. E., Macdougall, T. W., Birritta, F., Melnychuk, M. R., Molzan, K. M., et al., "Field Evaluation of Dual-Ended, High Temperature, Hydrogen Tolerant Fiber Optic DTS Sensor with Compact Fiber Loop Assembly," World Heavy Oil Congress, pp. 577-581, 2011.

146. Westerwaal, R., Rooijmans, J., Leclercq, L., Gheorghe, D., Radeva, T., et al., "Nanostructured Pd–Au Based Fiber Optic Sensors for Probing Hydrogen Concentrations in Gas Mixtures," International Journal of Hydrogen Energy, Vol. 38, No. 10, pp. 4201-4212, 2013.

147. Jiang, J., Ma, G.-M., Li, C.-R., Song, H.-T., Luo, Y.-T., et al., "Highly Sensitive Dissolved Hydrogen Sensor Based on Side-Polished Fiber Bragg Grating," IEEE Photonics Technology Letters, Vol. 27, No. 13, pp. 1453-1456, 2015.

148. Poole, Z., Ohodnicki, P., Yan, A., Lin, Y., and Chen, K., "Sub-CM Resolution Distributed Fiber Optic Hydrogen Sensing with Nano-Engineered TiO_2," ArXiv Preprint, 2015.

149. Huang, P.-C., Chen, Y.-P., Zhang, G., Song, H., and Liu, Y., "Note: Durability Analysis of Optical Fiber Hydrogen Sensor Based on Pd-Y Alloy Film," Review of Scientific Instruments, Vol. 87, No. 2, Paper No. 026104, 2016.

150. Zhu, H.-H., Shi, B., Yan, J.-F., Zhang, J., Zhang, C.-C., et al., "Fiber Bragg Grating-Based Performance Monitoring of a Slope Model Subjected to Seepage," Smart Materials and Structures, Vol. 23, No. 9, Paper No. 095027, 2014.

151. Jaroszewicz, L. R., Krajewski, Z., and Swillo, R., "Application of Fiber-Optic Sagnac Interferometer for Detection of Rotational Seismic Events," Molecular and Quantum Acoustics, Vol. 22, pp. 133-134, 2001.

152. Tyler, S., Holland, D., Zagorodnov, V., Stern, A., Sladek, C., et al., "Using Distributed Temperature Sensors to Monitor an Antarctic Ice Shelf and Sub-Ice-Shelf Cavity," Journal of Glaciology, Vol. 59, No. 215, pp. 583-591, 2013.

153. Rosolem, J. B., Dini, D. C., Penze, R. S., Floridia, C., Leonardi, A. A., et al., "Fiber Optic Bending Sensor for Water Level

Monitoring: Development and Field Test: A Review," IEEE Sensors Journal, Vol. 13, No. 11, pp. 4113-4120, 2013.

154. Li, H.-N., Li, D.-S., and Song, G.-B., "Recent Applications of Fiber Optic Sensors to Health Monitoring in Civil Engineering," Engineering Structures, Vol. 26, No. 11, pp. 1647-1657, 2004.

155. Roh, H. D., Lee, H., and Park, Y.-B., "Structural Health Monitoring of Carbon-Material-Reinforced Polymers Using Electrical Resistance Measurement," Int. J. Precis. Eng. Manuf.-Green Tech., Vol. 3, No. 3, pp. 311-321, 2016.

156. Li, D., Ho, S.-C. M., Song, G., Ren, L., and Li, H., "A Review of Damage Detection Methods for Wind Turbine Blades," Smart Materials and Structures, Vol. 24, No. 3, Paper No. 033001, 2015.

157. Wei, L., Zhou, Z.-D., Huang, J., and Tan, Y.-G., "FBG-Based Non-Contact Vibration Measurement and Experimental Study," Int. J. Precis. Eng. Manuf., Vol. 14, No. 9, pp. 1577-1581, 2013.

158. Di Sante, R., "Fibre Optic Sensors for Structural Health Monitoring of Aircraft Composite Structures: Recent Advances and Applications," Sensors, Vol. 15, No. 8, pp. 18666-18713, 2015.

159. Nicolas, M. J., Sullivan, R. W., and Richards, W. L., "Large Scale Applications Using FBG Sensors: Determination of in-Flight Loads and Shape of a Composite Aircraft Wing," Aerospace, Vol. 3, No. 3, p. 18, 2016.

160. Kang, D., Kim, H.-Y., Kim, D.-H., and Park, S., "Thermal Characteristics of FBG Sensors at Cryogenic Temperatures for Structural Health Monitoring," Int. J. Precis. Eng. Manuf., Vol. 17, No. 1, pp. 5-9, 2016.

161. Li, T., Tan, Y., Han, X., Zheng, K., and Zhou, Z., "Diaphragm Based Fiber Bragg Grating Acceleration Sensor with Temperature Compensation," Sensors, Vol. 17, No. 1, p. 218, 2017.

162. Jia, P., Fang, G., Liang, T., Hong, Y., Tan, Q., et al., "Temperature-Compensated Fiber-Optic Fabry-Perot Interferometric Gas Refractive-Index Sensor Based on Hollow Silica Tube for High-Temperature Application," Sensors and Actuators B: Chemical, Vol. 244, pp. 226-232, 2017.

163. Sun, G., Cen, Y., Zhao, L., Wei, C., and Chung, Y., "Combined Sagnac and Intermodal Interferences for Discrimination of Strain and Temperature Variations," Proc. of the 25th International Conference in Optical Fiber Sensors, pp. 1-4, 2017.

164. Zaghloul, M., Wang, M., Li, M.-J., Li, S., Milione, G., et al., "Dual-Core Optical Fibers for Simultaneous Measurements of Temperature and Strain Using Brillouin OTDA," Proc. of the Conference in Lasers and Electro-Optics, pp. 1-2, 2017.

165. Barrias, A., Casas, J. R., and Villalba, S., "A Review of Distributed Optical Fiber Sensors for Civil Engineering Applications," Sensors, Vol. 16, No. 5, p. 748, 2016.

166. Horta, A., Malone, B., Stockmann, U., Minasny, B., Bishop, T., et al., "Potential of Integrated Field Spectroscopy and Spatial Analysis for Enhanced Assessment of Soil Contamination: A Prospective Review," Geoderma, Vol. 241, pp. 180-209, 2015.

167. Sun, T., Fang, H., Liu, W., and Ye, Y., "Impact of Water Background on Canopy Reflectance Anisotropy of A Paddy Rice Field from Multi-Angle Measurements," Agricultural and Forest Meteorology, Vol. 233, pp. 143-152, 2017.

168. Martins, B. H., Araujo-Junior, C. F., Miyazawa, M., Vieira, K. M., and Milori, D. M., "Soil Organic Matter Quality and Weed Diversity in Coffee Plantation Area Submitted to Weed Control and Cover Crops Management," Soil and Tillage Research, Vol. 153, pp. 169-174, 2015.

169. Poggio, M., Brown, D. J., and Bricklemyer, R. S., "Laboratory-Based Evaluation of Optical Performance for A New Soil Penetrometer Visible and Near-Infrared (VisNIR) Foreoptic," Computers and Electronics in Agriculture, Vol. 115, pp. 12-20, 2015.

170. Senesi, G. S., Martin-Neto, L., Villas-Boas, P. R., Nicolodelli, G., and Milori, D. M., "Laser-Based Spectroscopic Methods to Evaluate the Humification Degree of Soil Organic Matter in whole Soils: A Review," Journal of Soils and Sediments, pp. 1-11, 2016.

171. Bense, V., Read, T., and Verhoef, A., "Using Distributed Temperature Sensing to Monitor Field Scale Dynamics of Ground Surface Temperature and Related Substrate Heat Flux," Agricultural and Forest Meteorology, Vol. 220, pp. 207-215, 2016.

172. Zhang, C.-C., Zhu, H.-H., and Shi, B., "Role of the Interface between Distributed Fibre Optic Strain Sensor and Soil in Ground Deformation Measurement," Scientific Reports, Vol. 6, Paper No. 36469, 2016.

173. Dooly, G., Manap, H., O'Keeffe, S., and Lewis, E., "Highly Selective Optical Fibre Ammonia Sensor for Use in Agriculture," Procedia Engineering, Vol. 25, pp. 1113-1116, 2011.

174. Laubach, J., Bai, M., Pinares-Patiño, C. S., Phillips, F. A., Naylor, T. A., et al., "Accuracy of Micrometeorological Techniques for Detecting a Change in Methane Emissions from a Herd of Cattle," Agricultural and Forest Meteorology, Vol. 176, pp. 50-63, 2013.

175. Huang, Y., Wieck, L., and Tao, S., "Development and Evaluation of Optical Fiber NH 3 Sensors for Application in Air Quality Monitoring," Atmospheric Environment, Vol. 66, pp. 1-7, 2013.

176. Goh, L. S., Anoda, Y., Kazuhiro, W., and Shinomiya, N., "Remote Management for Multipoint Sensing Systems Using Hetero-Core Spliced Optical Fiber Sensors," Sensors, Vol. 14, No. 1, pp. 468-477, 2013.

177. Tapetado, A., Díaz-Álvarez, J., Miguélez, M. H., and Vázquez, C., "Two-Color Pyrometer for Process Temperature Measurement during Machining," Journal of Lightwave Technology, Vol. 34, No. 4, pp. 1380-1386, 2016.

178. Díaz-Álvarez, J., Tapetado, A., Vázquez, C., and Miguélez, H., "Temperature Measurement and Numerical Prediction in Machining Inconel 718," Sensors, Vol. 17, No. 7, p. 1531, 2017.

179. Tapetado, A., Díaz-Álvarez, J., Miguélez, H., and Vázquez, C., "Fiber-Optic Pyrometer for Very Localized Temperature Measurements in a Turning Process," IEEE Journal of selected topics in Quantum Electronics, Vol. 23, No. 2, pp. 278-283, 2017.

180. Mandal, S., Roy, S., Chatterjee, K., Haldar, S., Vijay, V., et al., "Fiber Bragg Grating Sensor for Cutting Speed Optimization and Burr Reduction in Micro-Nano Scratching," Procedia Technology, Vol. 19, pp. 327-332, 2015.

181. Yao, S., Xu, J., Zhao, J., Bai, K., Lu, J., et al., "Characterization of Fly Ash Laser-Induced Plasma for Improving the On-Line Measurement of Unburned Carbon in Gas-Solid Flow," Energy & Fuels, Vol. 31, No. 5, pp. 4681-4686, 2017.

182. Wu, J., Wang, R., Pu, G., and Qi, H., "Integrated Assessment of Exergy, Energy and Carbon Dioxide Emissions in an Iron and Steel Industrial Network," Applied Energy, Vol. 183, pp. 430-444, 2016.

183. Hunsinger, G. B., Tipple, C. A., and Stern, L. A., "Gaseous Byproducts from High-Temperature Thermal Conversion Elemental Analysis of Nitrogen-and Sulfur-Bearing Compounds with Considerations for δ2H and δ18O Analyses," Rapid Communications in Mass Spectrometry, Vol. 27, No. 14, pp. 1649-1659, 2013.

184. Pospíšilová, M., Kuncová, G., and Trögl, J., "Fiber-Optic Chemical Sensors and Fiber-Optic Bio-Sensors," Sensors, Vol. 15, No. 10, pp. 25208-25259, 2015.

185. Tan, Y., Zhang, C., Jin, W., Yang, F., Ho, H. L., et al., "Optical Fiber Photoacoustic Gas Sensor with Graphene Nano-Mechanical Resonator as the Acoustic Detector," IEEE Journal of Selected Topics in Quantum Electronics, Vol. 23, No. 2, pp. 1-11, 2017.

186. Chen, H., Zhang, S., Fu, H., Li, H., Zhang, D., et al., "Fiber-Optic Temperature Sensor Interrogation Technique Based on an Optoelectronic Oscillator," Optical Engineering, Vol. 55, No. 3, pp. 031107-031107, 2016.

187. Xu, O., Zhang, J., Deng, H., and Yao, J., "Dual-Frequency Optoelectronic Oscillator for Thermal-Insensitive Interrogation of a FBG Strain Sensor," IEEE Photonics Technology Letters, Vol. 29, No. 4, pp. 357-360, 2017.

188. Ertman, S., Lesiak, P., and Woliński, T. R., "Optofluidic Photonic Crystal Fiber-Based Sensors," Journal of Lightwave Technology, Vol. 35, No. 16, pp. 3399-3405, 2017.

189. Zheng, Y., Chen, L. H., Yang, J., Raghunandhan, R., Dong, X., et al., "Fiber Optic Fabry–Perot Optofluidic Sensor with a Focused Ion Beam Ablated Microslot for Fast Refractive Index and Magnetic Field Measurement," IEEE Journal of selected topics in Quantum Electronics, Vol. 23, No. 2, pp. 1-5, 2017.

190. Alexander Schmidt, M., Argyros, A., and Sorin, F., "Hybrid Optical Fibers–An Innovative Platform for In-Fiber Photonic Devices," Advanced Optical Materials, Vol. 4, No. 1, pp. 13-36, 2016.

191. Villatoro, J. and Zubia, J., "New Perspectives in Photonic Crystal Fibre Sensors," Optics & Laser Technology, Vol. 78, pp. 67-75, 2016.